Water Research 272 (2025) 122902

Contents lists available at ScienceDirect

Water Research

journal homepage: www.elsevier.com/locate/watres

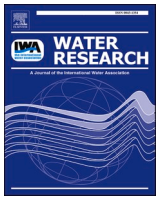

Ultrafiltration and composite microfiltration biocatalytic membrane activity and steroid hormone micropollutant degradation at environmentally relevant concentrations

Alessandra Imbrogno [a], Martin Schmidt [b], Agnes Schulze [b], María Teresa Moreira [c], Andrea I. Schäfer [a,*]

[a] Institute for Advanced Membrane Technology (IAMT), Karlsruhe Institute of Technology (KIT), Hermann-von-Helmholtz-Platz 1, 76344 Eggenstein-Leopoldshafen, Germany
[b] Leibniz Institute of Surface Engineering (IOM), Leipzig, Germany
[c] CRETUS, Department of Chemical Engineering, University of Santiago de Compostela, 15782, Santiago de Compostela, Spain

ARTICLE INFO

Keywords:
Laccase
Enzyme reaction kinetics
Ultrafiltration
ABTS
Estrogen oxidation
Physico-chemical water treatment

ABSTRACT

Biocatalytic degradation of micropollutants has been extensively explored in both batch and membrane reactors in μg/L to mg/L concentrations and variable water compositions. The degradation of micropollutants by biocatalytic membranes at environmentally relevant concentrations of ng/L range found in natural surface water matrices has not yet been investigated, presumably because of the challenging concentration analysis.

This study investigated the limitations of biocatalytic degradation of estradiol (E2) micropollutant at environmentally relevant concentrations by a biocatalytic membrane. The contributions of solute flux, hydraulic residence time (HRT) and water matrix composition on reaction kinetics, the apparent rate of disappearance (or reaction rate) and enzyme activity were examined. Two biocatalytic membranes were used: i) laccase entrapped in an ultrafiltration (UF) membrane support (namely UF-SNPs) and, ii) laccase covalently bound to the nanofiber matrix of a composite microfiltration (MF) membrane.

The three main findings are reported. Firstly, the apparent rate of E2 disappearance decreases significantly by four orders of magnitude at a low micropollutant concentration of 0.1 μg/L, resulting in undetectable degradation during filtration, irrespective of the biocatalytic membrane. Secondly, the solute mass transfer and HRT control the biocatalytic degradation through the membranes resulting in different E2 removal. For the UF-SNPs membrane, a removal of 31 % is achieved only by increasing the concentration to 3000 μg/L and at a flux of 60 $L/m^2.h$ (HRT of 4.5 s) due to an increase in solute flux by an order of magnitude similar to the apparent rate of disappearance. In contrast, the nano-MF membrane is ineffective in achieving biocatalytic degradation regardless of E2 concentration, as the HRT is approximately seven times lower (0.6 s) than that of the UF-SNPs, and thus insufficient for E2 to reach the catalytic site. Thirdly, the composition of the aqueous matrix plays a crucial role in the control of laccase activity irrespective of the membrane. Indeed, laccase is inactivated predominantly by chloride ions in synthetic carbonate buffer, since the typical NaCl concentration is about two orders of magnitude higher than E2 concentration.

This study highlights that the slower kinetics achieved in the biocatalytic UF-SNPs and MF membranes are ineffective in removing steroid hormone micropollutants at realistic concentrations in surface water matrices. Further research is suggested to accelerate the reaction kinetics at such low concentrations and prolong the residence time within the membrane.

* Corresponding author.
E-mail address: Andrea.Iris.Schaefer@kit.edu (A.I. Schäfer).

https://doi.org/10.1016/j.watres.2024.122902
Received 7 October 2024; Received in revised form 29 November 2024; Accepted 1 December 2024
Available online 2 December 2024

1. Introduction

1.1. Degradation of steroid hormone micropollutants by enzymes

Steroid hormone (SH) micropollutants are endocrine disrupting chemicals found everywhere in surface waters (Bilal et al. 2021). This is of great concern, as their interference with the endocrine systems of biota and humans has been identified at concentrations as low as 1 ng/L (Adeel et al. 2017, Wu et al. 2021). In the human body, SHs are metabolised through reduction, hydroxylation and conjugation reactions, catalysed by enzymes, such as reductase, mono-oxygenase (e.g. cytochrome), glucuronidase and sulfotransferase (Charni-Natan et al. 2019, Strott 2002). Inspired by nature, biocatalytic membranes are used in water treatment, where micropollutants are degraded by enzymes contained in fungi or bacteria (Khanzada et al. 2020, Nure and Nkambule 2023).

Oxidative enzymes extracted from plants and fungi, such as laccase, tyrosinase (with O_2 as electron acceptor) and peroxidase (with H_2O_2 as electron acceptor), are the most commonly used enzymes in water treatment to oxidize phenolic micropollutants, including estrogens (Barbhuiya et al. 2022, Morsi et al. 2020, Shakerian et al. 2020). Laccases from fungi are preferred to bacteria because they are extracellular, which facilitates the extraction, and the enzymes have about 20 times higher activity than those from bacteria, which is promising for degradation of micropollutants (Margot et al. 2013). Laccase is preferable to peroxidase and tyrosinase because (i) oxidation occurs without the addition of peroxide (in the case of peroxidase) and (ii) the redox potential (0.5 to 0.8 V) is higher compared to tyrosinase (-0.3 V). This indicates that laccase is a stronger oxidant (Beck et al. 2018, Ghosh and Mukherjee 1998). Previous studies reported the oxidation of estrogens (estrone, 17β-estradiol, 17α-ethinylestradiol, estriol) by laccase mostly in batch reactors (Auriol et al. 2007, Liu et al. 2021, Lloret et al. 2010), immobilised on a nanofiber matrix (Rybarczyk et al. 2023, Zdarta et al. 2022a), and combined with ultra or nanofiltration (UF/NF), where the membrane is used as a barrier to retain the enzyme in the solution (Asif et al. 2018, Asif et al. 2020, Lloret et al. 2013b, Nguyen et al. 2015). A first attempt to develop a biocatalytic membrane where laccase is immobilised on a polyelectrolyte multilayer membrane for the degradation of ethinylestradiol (0.1 mg/L) during filtration has been published (Zdarta et al. 2022c).

1.2. Biocatalytic degradation mechanism of steroid hormones by laccase

Laccase from white-rot fungi contains a catalytic site with four coppers in the oxidation state 2^+, namely one type-1 (T1-Cu), one type-2 (T2-Cu) and two type-3 (T3-Cu) (see Fig. 1A) (Wang and Chen 2019). The catalytic reaction occurs through the oxidation of four phenol groups (i.e. four estradiol molecules) by T1-Cu and the subsequent transfer of four electrons and H^+ to the trinuclear T2/T3-Cu group, which reduces molecular oxygen to two water molecules (Catherine et al. 2016, Sun et al. 2021). Phenoxy radicals are the products generated from the oxidation reaction of estradiol. These radicals can react with each other through phenolic condensation or coupling, forming polymeric products, such as dimers or oligomers (molecular weight up to 1.8 kDa) with negligible estrogenic activity (Beck et al. 2018, Catherine et al. 2016). A previous study reported that the first electron transfer from the phenol group to the T1-Cu copper of laccase is the limiting step of the oxidation reaction, controlled by the redox potential difference between phenol and the T1-Cu site of laccase (Xu 1996). A higher redox potential indicates a faster reaction rate.

1.3. Biocatalytic membrane design, kinetics and mass transfer limitation

In nature, enzymes are usually entrapped in biological membranes and several attempts have been made to reconstruct this compartmentalization with synthetic membranes to perform enzymatic reactions (Küchler et al. 2016, Mazzei et al. 2024, Omidvar et al. 2021). In water treatment, biocatalytic degradation of micropollutants is combined with a single-step membrane filtration (Kumar et al. 2020). This is advantageous as it allows the in-situ removal of micropollutants, while filtering

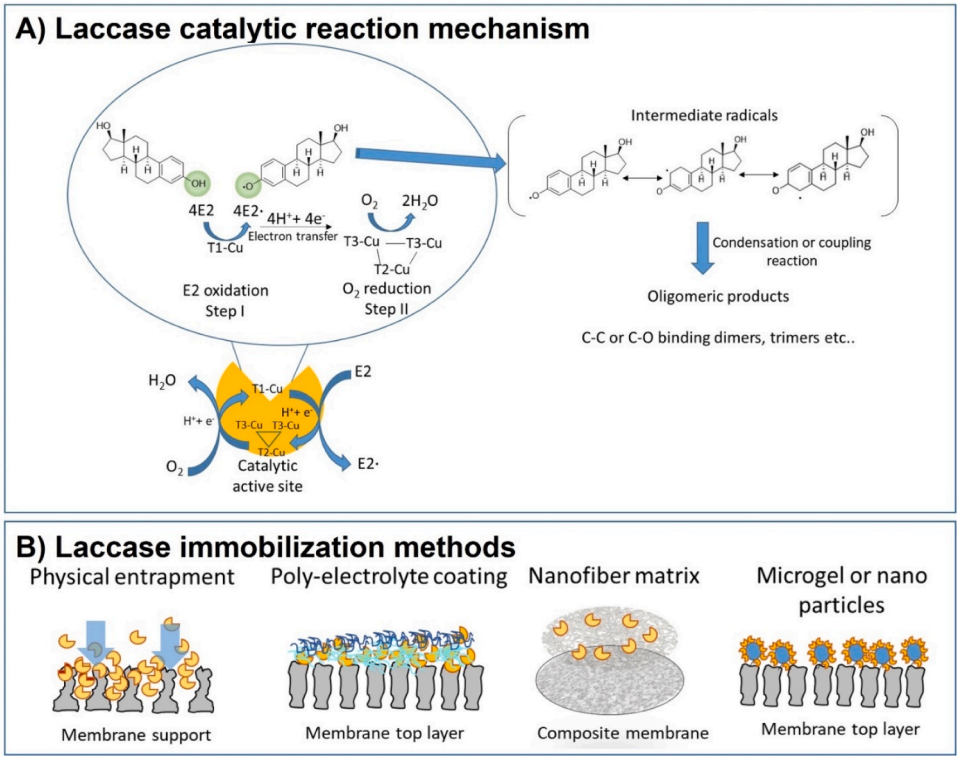

Fig. 1. A) Mechanism of biocatalytic oxidation of estradiol by laccase, B) Methods of enzyme immobilization in water filtration membranes.

water without concentrating these pollutants in the waste stream (Kujawska et al. 2022, Luo et al. 2020, Morsi et al. 2020). Alternative emerging processes used for micropollutant degradation are advanced oxidation processes (e.g. photocatalytic and electrochemical membranes), where the production of oxygen reactive species occurs by light irradiation or electricity source (Kujawska et al. 2022). Although these processes can effectively remove micropollutants at environmental concentrations of ng/L (Lotfi et al. 2022, Lyubimenko et al. 2021), there are still some limitations that can be overcome by using biocatalytic membranes, such as: i) the damage of the polymeric membranes by both irradiation and reactive oxygen species, ii) the loss of photocatalytic activity due to limited light source penetration, and iii) the substantial energy demand in the form of light or electricity required to start the reaction (Hodges et al. 2018, Shi et al. 2019).

A schematic representation of the laccase immobilization methods applied for the degradation of micropollutants is depicted in Fig. 1B. Physical entrapment of the enzyme on a semi-permeable membrane support or within a polyelectrolyte coating layer are the most commonly used methods (Luo et al. 2020, Omidvar et al. 2021, Restrepo et al. 2024, Vitola et al. 2019, Zhang et al. 2021). Specific examples of biocompatible coating materials used for laccase immobilization, such as alginate, gelatine and catecholamine layer coatings (De Cazes et al. 2015, Dong et al. 2022, Marpani et al. 2015), layer-by-layer polyelectrolytes (Jankowska et al. 2022a, Li et al. 2020, Popkov et al. 2023, Restrepo et al. 2023, Zdarta et al. 2022c), and dopamine grafted coatings (Cao et al. 2018, Li et al. 2018, Zhang et al. 2021) are reported in Table S1. Alternative strategies for enzyme immobilisation include attachment to microgel particles (Bilal et al. 2019, Vitola et al. 2017) and polymer or ceramic nanomaterials, such as electrospun nanofiber and nanoparticles (Dai et al. 2016, Jankowska et al. 2023, Jankowska et al. 2022b, Jankowska et al. 2024, Moreira et al. 2017, Zdarta et al. 2020, Zhao et al. 2023). The electrospun particles or nanofibers increase the surface area where the enzyme can be covalently immobilised, thus providing higher enzyme loading compared to direct entrapment on a membrane surface (Luo et al. 2020). Enzyme loading on the membrane is an important factor controlling the reaction kinetics, as the reaction rate is directly proportional to the enzyme concentration (Bisswanger 2017).

In addition to enzyme concentration, other factors controlling reaction kinetics are substrate concentration (e.g. micropollutant) and solution chemistry. The relationship between reaction rate and substrate concentration is described by the Michaelis-Menten equation. This relationship indicates that the reaction rate increases with increasing substrate concentration until a maximum value is reached. At this maximum, all enzyme molecules are complexed with the substrate, consequently the enzyme becomes saturated (Punekar 2018). The reaction rate follows first-order kinetics at concentrations below the Michaelis-Menten constant (K_M, which is the substrate concentration at which the reaction rate is half of the maximum value), while it follows zero-order kinetics (hence, independent of substrate concentrations) at concentration above K_M (i.e. saturating conditions) (Bisswanger 2017). In a previous study (Auriol et al. 2007), K_M for different estrogens (estrone, estradiol, estriol and ethinyl-estradiol) was determined in a range of 2.6 to 3.9 μM (corresponding to 0.8 and 1.0 mg/L) in phosphate buffer.

Clearly, concentration is important, particularly for micropollutants, where low concentrations mean that mass transfer often limits degradation. At lower substrate concentrations, the reaction depends on molecular contact between enzyme and substrate, which is limited by diffusion mass transfer (Punekar 2018). The mass transfer limitation can be overcome to some extent by immobilization on membranes (Lyubimenko et al. 2021). In a biocatalytic membrane, in addition to the diffusion of the substrate through the bulk solution and the porous membrane structure, the reaction is influenced by convective mass transfer of the substrate (e.g. micropollutants) from the bulk solution to the enzymatic catalytic active site (Nagy et al. 2012). This was confirmed in previous studies (Giorno et al. 2006, Gumí et al. 2008), where an increase in substrate conversion was observed when the water flux was increased. This increase was attributed to more substrate molecules reaching the biocatalytic active sites. In contrast, at low convective flux, diffusive mass transport of the substrate becomes the rate-limiting step in the reaction (Ansorge and Staude 1985).

1.4. Role of hydraulic residence time on enzyme kinetics in biocatalytic membranes

When performing a catalytic reaction in a membrane reactor, the hydraulic residence time (HRT) within the membrane can be a limiting factor for the kinetics of the reaction and, consequently, for the removal of micropollutants, as it affects the time for the substrate to reach the enzymatic catalytic site (Levenspiel 1998). Previous studies with either biocatalytic membranes (Ansorge and Staude 1985) or flow microreactor configurations (Cardinal-Watkins and Nicell 2011, Lloret et al. 2013a), reported that decreasing the HRT of the microreactor shortens the contact with the enzyme, making solute mass transport within the pores the reaction limiting step. In this case, adsorption of micropollutants on the membrane or adsorbent particles (e.g. activated carbon) can promote enzymatic degradation by prolonging the residence time of the contaminant on the membrane beyond the HRT and this enhanes the contact with the enzyme (Cao et al. 2016, Nguyen et al. 2016). At lower convective flux, hence longer HRT, the enzyme reaction rate increases until it becomes constant, indicating that the reaction is only dependent on diffusion mass transport at higher flux (Ansorge and Staude 1985). A similar observation has been reported in a previous study (Gebreyohannes et al. 2017), where the enzymatic reaction rate was investigated at substrate concentrations where the enzyme is saturated and, consequently, the reaction rate is no longer limited by variations in HRT. These studies indicate an interaction between micropollutant concentration and HRT in controlling the enzymatic reaction rate in a biocatalytic membrane. Although this has been investigated under enzyme saturation conditions (concentrated feed solution), it is relevant to further elucidate the role of HRT and solute mass transfer when micropollutants are at environmental concentrations (ng/L range), where the enzyme is unlikely to be saturated. In this case, the contact time between the contaminant and the enzyme is expected to be crucial in controlling enzymatic degradation and, consequently, micropollutant removal.

1.5. The challenge of enzymatic micropollutant degradation

Most biocatalytic membranes have been designed to treat wastewater effluents, where micropollutants are concentrated above 100 μg/L (Bilal and Iqbal 2019, Zdarta et al. 2021). In studies with batch reactors, removal of estrogens (e.g. estrone, 17β-estradiol, 17α-ethinylestradiol, estriol) in the range of 60 to 90 % has been achieved using laccase within 1 h of reaction (Auriol et al. 2007, Liu et al. 2021, Lloret et al. 2010). These studies verify the effectiveness of biocatalytic degradation by laccase when operating in batch mode (hence prolonged contact time) and using highly concentrated solutions. However, in surface waters, micropollutants are present at concentrations from 0.001 μg/L to 0.5 μg/L (Bilal et al. 2021, Schröder et al. 2016), which can pose a challenge for enzymatic degradation due to slower reaction kinetics (Rangelov and Nicell 2015, 2018). Previous kinetic studies in batch reactors revealed that, when estradiol concentration is decreased by one order of magnitude (from micro to nanomolar), laccase is predominantly in an oxidised state, which is not catalytically active, and micropollutant degradation requires a longer time (3 hours) to reach full removal (Rangelov and Nicell 2018). In another study (Cardinal-Watkins and Nicell 2011), a 4-fold reduction in estradiol concentration (from 20 to 5 μM) resulted in a 3-fold decrease in removal (from 60 to 20 %) in a bed column configuration, attributed to a decrease in reaction rate at lower concentration. These batch studies highlight that micropollutant concentration is a limiting factor for enzyme kinetics and it is relevant to

investigate micropollutant degradation at more realistic concentrations present in natural and wastewaters. Although effective removal (>85 %) was achieved by a biocatalytic membrane for highly concentrated (0.01 to 5 mg/L) estrogen solutions (Zdarta et al. 2022c), no studies are reported to assess the biocatalytic degradation during filtration, when estrogens are present at low water concentrations of ng/L. In this case, the enzymatic kinetics is expected to play an important role in controlling the micropollutant degradation during the relatively short hydraulic residence times within the membrane.

In addition to micropollutant concentration, the composition of the aqueous matrix can affect biocatalytic degradation. In fact, it has been reported that testing biocatalytic reactions with buffers (e.g. phosphate and acetate buffers), that are not representative of the natural water composition, may result in an overestimation of enzymatic activity and the reaction rate (Cardinal-Watkins and Nicell 2011, Maryskova et al. 2021). Some examples are summarized in Table S1. Several studies found variable micropollutant removal in the range of 36 to 80 %, when biocatalytic degradation is tested in real water and wastewater conditions (Jahangiri et al. 2018, Lloret et al. 2013b, Maryskova et al. 2021, Rybarczyk et al. 2023, Zdarta et al. 2022b), while removal above 80 % has been observed with laccase when tested in synthetic buffer (see Table S1). The high variability of elimination depends on the composition of the water matrix, where the presence of enzyme inhibitors (e.g. salts, metals, solvents) may interfere with enzyme kinetics and ultimately with removal (Rybarczyk et al. 2023, Zdarta et al. 2022b). A low removal of 35 to 40 % of estrogens by laccase oxidation has been reported using real wastewater (Rybarczyk et al. 2023), highlighting the importance of studying the biocatalytic degradation of micropollutants using a composition similar to natural water matrices.

1.6. Laccase inhibition by chloride ions and organic solvents

The presence of enzyme inhibitors, which can bind to the laccase catalytic site or the enzyme-pollutant complex, is one crucial factor for the lower efficiency of micropollutant degradation in real water matrix compositions. Among various inhibitors, inorganic salts (e.g. sodium chloride) and solvents are the most common, and their inhibition depends on salt and solvent types as well as concentration (Chapple et al. 2019, Zdarta et al. 2022b). A fourfold reduction in the reaction rate with an increase in chloride ion concentration up to 50 mM has been observed in a previous study (Raseda et al. 2014). The inhibition has been attributed to the reversible binding of chloride ions to the laccase catalytic active site. Similarly, a 20 % reduction of the reaction rate was found at chloride concentrations below 5 mM (Margot et al. 2013). Regarding solvent inhibition, it was reported that polar organic solvents (e.g. acetone, methanol, ethanol) can reduce the laccase reaction rate by 10 %, when used at fractions below 10 % (Kim and Nicell 2006). A molecular dynamic simulation study demonstrated that inhibition by polar organic solvents (such as ethanol) is attributed to weak hydrogen bonding interactions with the amino acids of laccase (Jafari et al. 2020). These weak interactions replace the water molecules in the enzyme hydration shell with solvent molecules, altering the laccase structure (Jafari et al. 2020). Further investigation is required to elucidate the significance of laccase inhibition when the enzyme is used in a biocatalytic membrane to degrade micropollutants at environmental concentrations of ng/L, where the pollutant concentration is likely to be several orders of magnitude lower than the salt (order of g/L) or solvent (mg/L) concentrations.

The present study aims to provide novel insights into the enzymatic kinetics and the limitations of steroid hormone micropollutant degradation using biocatalytic membranes at environmental concentrations and electrolyte background similar to natural water compositions. The contribution of solute mass transfer, water matrix and HRT on the enzymatic kinetics and ultimately, the steroid hormone removal is evaluated to answer three main research questions: i) which factors limit the degradation of steroid hormone micropollutants at environmentally relevant concentration by biocatalytic membranes (e.g. kinetics, solute flux, water matrix)? ii) is the enzyme kinetics compatible with the HRT in a biocatalytic membrane operated at micropollutant environmental concentration of ng/L? iii) what is the contribution of the water matrix composition on the biocatalytic membrane activity and kinetics? Two biocatalytic membranes with immobilized laccase were prepared (i) as a nanobiocatalyst into an ultrafiltration (UF) membrane support and, (ii) in a microfiltration (MF) nanofiber composite membrane. This provided different ranges of HRT within the membrane at similar water flux. The results are expected to identify the limiting factors for the biocatalytic degradation of steroid hormone micropollutants under realistic environmental concentrations and synthetic water matrices.

2. Materials and methods

2.1. Biocatalytic membrane design

Two biocatalytic membranes were designed to provide: i) a different spatial location of the enzyme in the membrane (entrapped within the support or attached on the membrane surface directly in contact with the feed solution), and ii) different ranges of HRT (hence contact time) typically used in UF and MF membranes operated at variable water flux. One biocatalytic membrane reactor consisted of a composite UF membrane with a nanobiocatalyst (enzyme + silica nanoparticles, namely SNPs) entrapped in a sandwich configuration (UF-SNPs) (Fig. 2A, B, C). The second biocatalytic membrane reactor comprised a nanofiber composite MF membrane, namely nano-MF, where the enzyme was covalently attached by electron beam irradiation and subsequent chemical coupling in the nanofiber matrix (Fig. 2 D, E, F). The biocatalytic membrane reactors provided similar enzyme loadings of 3 and 2 g/m^2 for the nano-MF and UF-SNPs, respectively, (see Table S6), while the range of HRT was more than 10 times higher in the UF-SNPs (4.5 s to 0.2 s) compared to the nano-MF (0.6 s to 0.03 s), when operated at similar flux values (see Figure S7). HRT was calculated considering the UF support thickness (where the nanobiocatalyst was entrapped) and the nanofiber matrix thickness with the enzyme covalently attached (see Eq. S2). In the case of nano-MF, HRT was calculated considering the nanofiber matrix thickness, where most of laccase was expected to be immobilized by electron beam and chemical coupling, although a minimal binding to the MF support cannot be excluded. The larger HRT in the UF-SNPs is related to a higher thickness of the UF membrane support (150 μm in Table 1) compared to the nanofiber matrix thickness (15 ± 4 μm) estimated from SEM images shown in Figure S3. The different range of HRT is expected to contribute significantly to the contact between the micropollutant and the enzyme, and consequently the removal.

Two different supports were used for the biocatalytic membranes to retain the nanobiocatalyst within the membrane (in the case of the UF-SNPs) and to provide negligible adsorption of steroid hormones, which can obscure removal by enzymatic degradation. A UF regenerated cellulose membrane (Ultracel PLHHK, Millipore, USA) with a molecular weight cut off (MWCO) of 100 kDa was used for the UF-SNPs membrane preparation. For the nano-MF, a hydrophilic microfiltration polyvinylidene fluoride membrane (MF GVPP-PVDF, Millipore, USA) was used for the deposition of an electrospun PVDF nanofiber matrix. The membrane characteristics (e.g. porosity, membrane thickness and mean pore diameter) are listed in Table 1.

2.2. Materials

Laccase from *Trametes versicolor* (Lac Trv, Sigma Aldrich, specific activity ranges 0.5 to 1.4 μMol/min.mg from manufacturer) was the enzyme used for the biocatalytic membrane preparation, as the oxidation of estrogens has been demonstrated in the literature (Beck et al. 2018). Fumed silica nanoparticles (SNPs, Sigma Aldrich, average diameter of of 0.2-0.3 μm from the manufacturer) were used for Lac Trv immobilisation and nanobiocatalyst preparation. Silica was selected due

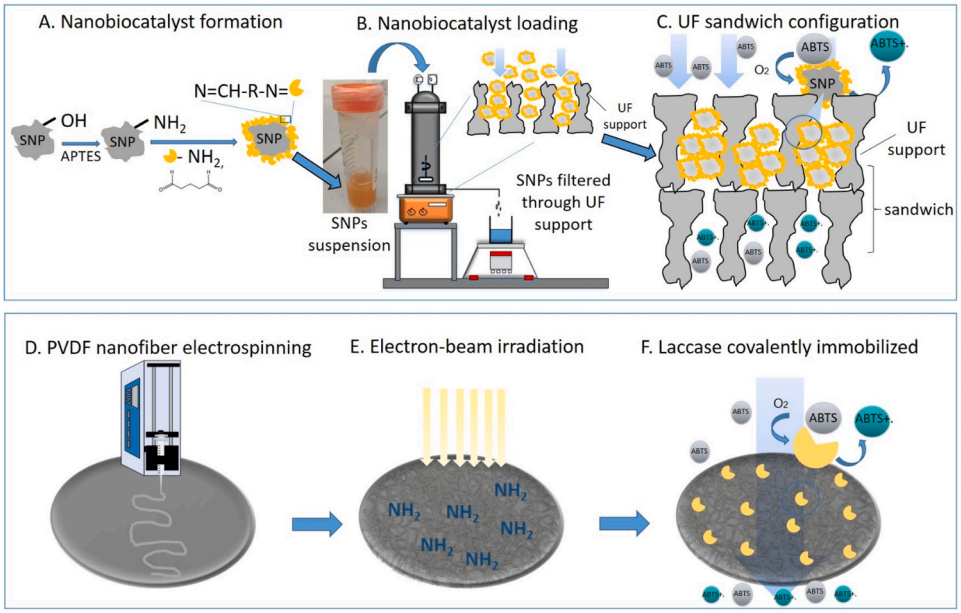

Fig. 2. Schematic of UF-SNPs (A, B, C) and nano-MF (D, E, F) membrane design and preparation steps.

Table 1
Membrane type, materials, porosity and thickness.

Membrane type	Material	Porosity	Support thickness (μm) [a]	Membrane thickness (μm)[d]	Mean pore diameter (μm)	Ref.
UF	Regenerated cellulose support: polypropylene	0.5	150	230	0.018[b]	(Nguyen et al. 2021)
MF-PVDF	Polyvinylidene-fluoride	0.7	–	130	0.2[c]	(Lyubimenko et al. 2021)

[a] estimated from FESEM images of support thickness reported by (Nguyen et al. 2021),
[b] calculated as the equivalent sphere diameter of MWCO using $D=2\bullet2.0374\ 10^{-11}\ MW^{0.53}$ (Worch and E. 1993),
[c] from manufacturer,
[d] including support and dense skin layer for UF

to its chemical and thermal stability and its previous application in laccase immobilisation (Moreira et al. 2017). Amino groups on the SNPs particles and cross-linking with Lac Trv was performed with 3-aminopropyltriethoxysilane (APTES, Alfa Aesar, purity 98 %) and glutaraldehyde (GA, Grade II, 25 % in water, Sigma Aldrich, Germany), respectively. The electrospun nanofiber matrix was prepared using N, N-dimethylformamide (DMF, 99 %, Sigma-Aldrich, Germany) as a solvent and PVDF (1015/1001, Solvay, Belgium) as polymer. The coupling of Lac Trv with the PVDF nanofiber was performed using 2-aminoethylmethacrylamide hydrochloride (AEMA, purchased from Sigma Aldrich) during electron-beam-induced grafting. For the covalent bonding with the aminated PVDF nanofiber matrix, 1-ethyl-3-(3-dimethylaminopropyl) carbodiimide hydrochloride (EDC, Sigma Aldrich) and *N*-hydroxysuccinimide (NHS, Sigma Aldrich) were used. To determine Lac Trv activity, 2,2′-azino-bis(3-ethylbenzothiazoline-6-sulfonic acid) diammonium salt (ABTS, Thermo Fisher, MW 548.7 g/mol) was used, as it is reported to be the substrate model for determining Lac Trv activity (Bourbonnais et al. 1998). ABTS as well as E2 feed solutions were prepared with two different water matrices: i) a phosphate buffer composed of disodium phosphate (Na_2HPO_4) and citric acid monohydrate ($C_6H_8O_7$, 99.9 %, VWR, Germany) 0.1 M, commonly used to evaluate enzyme activity, and ii) a synthetic carbonate buffer composed of sodium chloride (NaCl 10 mM, VWR Chemicals, Germany) and sodium carbonate ($NaHCO_3$ 1 mM, Bernd Kraft, Germany, 99.7 % purity) to reproduce a natural water background.

2.3. Nanobiocatalyst preparation and loading into the UF membrane

The nanobiocatalyst (SNPs + Lac Trv) was prepared by cross-linking Lac Trv with the amino-functionalised SNPs using a method reported in previous studies (Moreira et al. 2017, Zimmermann et al. 2011). The reaction mechanism is shown in Fig. 2A. The amino groups were created on SNP particles by adding APTES at a concentration of 4.3 μMol/g to an SNP's suspension of 10 g/L dissolved in a disodium phosphate solution ($Na_2HPO_4\bullet H_2O$, Merck Millipore, Germany) 0.1 M and pH 7. The reaction was carried out for 24 hours in a shaker at 150 rpm and 20 °C. The bonding of Lac Trv to the amino groups of the SNP particles was subsequently achieved by adding GA 1 mmol/g and a specific volume of Lac Trv to obtain a final enzyme concentration of 1.2 g/L (from a Lac stock solution of 200 g/L) and activity of 20,000 μMol/min.L. The cross-linking reaction was performed in a shaker for 1 hour at 150 rpm and 20 °C (see Table S3 for detailed description of the reaction method). Different APTES, GA, and Lac Trv concentrations were tested to find the optimal conditions for Lac immobilisation (see Figure S1 and S2). A specific nanobiocatalyst activity of 2.1 ± 0.3 μmol/min.mg was obtained, which is similar to the specific activity obtained in a previous study (2.6 μMol/min.mg) (Moreira et al. 2017) using similar SNP particles and immobilisation method.

The nanobiocatalyst was loaded into the UF membrane support, following a method from a previous study (Nguyen et al. 2021). A nanobiocatalyst suspension of 0.2 g/L was prepared by adding 3.2 mL of stock solution 20 g/L (activity 25,500 μmol/min.L) to 320 mL of disodium phosphate solution 0.1 M, pH 7. The suspension was filtered in a stainless-steel dead-end cell at 1 bar with the UF membrane support

layer facing the solution and a membrane area of 38.5 cm^2 (Fig. 2). The filtration was performed under unstirred conditions to allow a uniform deposition of the nanobiocatalyst particles onto the support until the entire feed volume was permeated. The UF sandwich configuration (Fig. 2C) was obtained by adding another UF membrane underneath to prevent the loss of SNPs in the permeate during filtration. The UF membrane loaded with the nanobiocatalyst was stored in phosphate-buffered saline (PBS) solution 0.1 M, pH 7 and 4 °C.

2.4. Laccase immobilisation on the MF composite nanofiber membrane

The MF composite nanofiber membrane was prepared by electrospinning of 3 mL solution of PVDF (21 %, w/v) dissolved in DMF using a flow rate of 0.5 mL/h and a ¼ A4 PVDF MF membrane support sheet (Fig. 2D). The voltage was set at 15 kV and the distance from the collector was 20 cm. The description of the electrospinning system is reported in a previous study (Lin et al. 2024). The nanofiber diameter and the cross-section of the nanofiber matrix thickness were analysed by scanning electron microscopy (SEM, JEOL JSM-IT500 InTouchScope™) at an accelerating voltage of 15 kV after gold coating. The cross-section thickness was used to calculate the HRT in the matrix, which is the time during which contact between Lac and the substrate occurs.

Lac Trv immobilisation on the MF composite membrane was performed in two steps: i) amino functionalisation of the PVDF nanofiber matrix (Fig. 2E), and ii) covalent bonding of the membrane amino groups with the COOH groups of Lac Trv (Fig. 2F). The amino functionalisation was performed by electron beam-induced grafting of AEMA using a self-built electron accelerator at an acceleration voltage of 160 kV, beam current of 10 mA and N_2 atmosphere (Schmidt et al. 2018). The covalent coupling of Lac Trv with the aminated PVDF was performed using a solution containing an enzyme concentration of 10 g/L, 20 g/L of EDC and 2 g/L of NHS, following the conditions reported in previous studies (Jahangiri et al. 2014, Schmidt et al. 2018). The reaction was performed in a phosphate-buffered saline solution (PBS, 50 mM, pH 7.4 ± 0.2) for 16 hours at room temperature. The reaction steps are detailed in Table S4. The biocatalytic membranes were rinsed with water four times for 15 minutes each and stored in PBS solution at pH 7.4 ± 0.2 and 4 °C.

2.5. Determination of laccase activity during filtration

The catalytic activity of an enzyme is the variation in the reaction rate of a specific chemical reaction in an assay system. The activity is usually reported as the reaction rate (moles of substrate converted per unit time) normalised by the reactor volume. Laccase activity was determined for the free Lac Trv in the stock solution, SNPs suspension and the biocatalytic membrane to confirm enzyme functionality and evaluate whether the catalytic site was available for reaction after immobilisation in the membrane. The activity of the Lac Trv stock solution and SNPs suspension was determined in batch in a quartz cuvette and UV–vis and calculated with Eq. S1. The activity of the biocatalytic membrane during filtration was determined by calculating the apparent rate of ABTS disappearance. The apparent rate of disappearance during filtration (r'', mol/s.m^2) was determined from a mass balance in a continuous flow reactor as shown in Eq. (1) (Giorno et al. 2017, Levenspiel 1998):

$$\mathrm{IN} = \mathrm{OUT} + \mathrm{PROD} + \mathrm{ACC} = (Q{\cdot}c)_{IN} = (Q{\cdot}c)_{OUT} + (r''{\cdot}V) + \frac{dVc}{dt} \quad (1)$$

where $Q_{IN,\ OUT}$ and $c_{IN,OUT}$ are the flow rate (m^3/s) and concentration (mol/m^3) of the reactant in the feed and permeate side, respectively, and V is the reactor volume (m^3). From Eq. (1), r'' was normalised by the catalytic membrane area (A, m^2) and calculated with Eq. (2) (Lyubimenko et al. 2019), assuming that: i) no ABTS was retained in the feed side (ACC=0), ii) the filtration system was operated at a constant feed flow rate ($Q_f = Q_p$) (Giorno et al. 2017).

$$r'' = \frac{Q_p\ (c_f - c_p)}{A} \quad (2)$$

where Q_p is the permeate flow rate (m^3/min) and $c_{f,p}$ (μmol/m^3) is the ABTS concentration in the feed and permeate, respectively. Considering that the filtration system was operated in flow-through mode and ABTS (Mw is 0.55 kDa) was not retained by the UF (MWCO of 100 kDa) and the MF membrane based on size exclusion, the assumptions to apply Eq. (2) are valid.

To determine the biocatalytic membrane activity during filtration, a feed solution containing different concentrations of ABTS from 0.5 to 0.001 mM was filtered through the membrane in a micro cross-flow system (micro-CF) operating in flow-through mode (with the retentate side closed) at a fixed flow rate of 0.65 mL/min and a biocatalytic membrane area of 2 cm^2. A schematic of the micro-CF system is shown in Figure S4 and a description of the system characteristics is reported in a previous study (Imbrogno and Schäfer 2019). Details of the filtration protocol are reported in Table S7.

ABTS solutions were prepared in phosphate and carbonate buffer (NaCl-$NaHCO_3$) at pH 3 ± 0.2, as this is reported to be the optimal pH for the reaction of ABTS with Lac Trv (Raseda et al. 2014). The depletion of ABTS concentration in the feed and permeate side was monitored by measuring the absorbance of aqueous samples with a UV–vis spectrophotometer (Perkin Elmer Lambda 365) at a wavelength of 340 nm. The concentration was calculated using the extinction coefficient obtained from the calibration curve. The latter was determined by measuring the absorbance of different ABTS concentrations in a range from 0.0006 up to 0.1 mM (calibration and limit of detection are shown in Figure S5).

2.6. Determination of enzyme kinetics with the Michaelis-Menten equation

The enzymatic kinetic was investigated to determine the contribution of different water matrices on the reaction rate and Lac affinity, which is defined as the strength of the binding between the substrate and enzyme catalytic site (Punekar 2018). The enzyme kinetics is described by the Michaelis-Menten equation, Eq. (3), where three kinetic parameters can be determined: i) the maximum apparent rate of disappearance (r''_{max}, mol/s), which is the highest reaction rate achievable when the enzyme is fully saturated by the substrate, ii) the Michaelis -Menten constant (K_M, M), which is defined as the ABTS concentration providing half of the maximum reaction rate and is a measure of enzyme affinity, iii) the reaction rate constant (K_r, 1/s) as a first-order kinetic reaction from the ratio $r''_{max}/\ K_M$. These parameters are determined by plotting the reaction rate r''(mol/s) as a function of ABTS concentrations (c_{ABTS}, M) in the feed (Bisswanger 2017):

$$r'' = \frac{r''_{max}{\cdot}c_{ABTS}}{K_M + c_{ABTS}} \quad (3)$$

At higher K_M values, the affinity for ABTS is reduced (Bisswanger 2017). The Michaelis-Menten equation is based on several assumptions: i) one ABTS molecule is converted into a product, ii) the product formation is proportional to the ABTS-Lac complex formation, iii) the ABTS-Lac complex depends on ABTS concentration, iv) the reaction reaches steady-state at enzyme saturating conditions (Bisswanger 2017). A linearised form of Eq. (3) gives the Lineweaver–Burk equation Eq. (4), which is used to estimate K_M from the slope (K_M/r''_{max}) and $1/r''_{max}$ from the intercept by plotting the inverse of r'' versus the inverse of c_{ABTS} (Drioli and Giorno 2010):

$$\frac{1}{r''} = \frac{K_M}{r''_{max}}\cdot\frac{1}{c_{ABTS}} + \frac{1}{r''_{max}} \quad (4)$$

2.7. Steroid hormone micropollutants and water matrix

Radiolabeled [2,4,6,7-^{3}H] estrone (E1, 3.48 TBq/mM), [2, 4, 6, 7–3H] β-estradiol (E2, 2.59 TBq/mM), [1,2,6,7-^{3}H] progesterone (P, 3.63 TBq/mM), and [1,2,6,7-^{3}H] testosterone (T, 2.94 TBq/mM) (purchased from Perkin Elmer USA) were used in ethanol solution with an activity of 37 MBq/mL, corresponding to 1 mCi. Batch and filtration experiments were performed with E2 as representative steroid hormone micropollutant, because it is reported in the watch list of the 2022 European Commission (European Parliament Commission implementing decision (EU), 2022) and is effectively oxidised by Lac Trv (Beck et al. 2018). T, E1 and P were used to evaluate biocatalytic degradation during filtration in phosphate buffer and the results are shown in Figure S9. E2 solutions were prepared using the synthetic carbonate buffer (NaCl-$NaHCO_3$) and phosphate buffer at pH 5.0 ± 0.1. This pH was selected as it is within the range of optimal pH (4–6) for the oxidation of estrogens with Lac Trv (Auriol et al. 2007, Lloret et al. 2010). E2 concentration in the solution was varied from 0.1 μg/L, which is representative of steroid hormone concentration in surface water (ranging from 0.001 μg/L up to 0.5 μg/L) (Bilal et al. 2021, Schröder et al. 2016) to 3000 μg/L, which is close to E2 solubility limit in water (3900 μg/L) (Shareef et al. 2006). For E2 concentrations above 100 ng/L (0.1 μg/L), a fixed volume (10 % v/v) of non-labeled E2 stock of 1, 5, 10 and 30 mg/L in methanol was added to the radiolabeled E2 solutions (100 ng/L).

2.8. Steroid hormone micropollutant analysis

To determine the total tritium (H^3) concentration from non-degraded hormone molecules, oligomeric products and free H^3, a liquid scintillation counter (LSC, 4910 TR, Perkin Elmer, USA) was used. The analysis was performed by mixing 1 mL of aqueous hormone solution with 1 mL of a scintillation cocktail (Ultima Gold LLT, Perkin Elmer, USA) (Bridle et al. 2016). To quantify the concentration of the oxidised steroid hormones molecules by the enzyme, their concentration was measured with ultra-high performance liquid chromatography combined with a flow scintillation analysis (UHPLC-FS) (Lyubimenko et al. 2020), where the depletion of the hormone peak area caused by the enzymatic degradation was quantified. A calibration curve with standard concentrations was determined for LSC and UHPLC-FS to calculate hormone concentration. The calibration curves and the limit of detection are shown in Figure S6.

2.9. Determination of steroid hormone degradation in batch experiments and kinetics

E2 degradation by the nanobiocatalyst was assessed in batch to determine the reaction rate and the kinetic parameters (r''_{max}, K_M and K_r) in a range of concentrations from 0.1 μg/L up to values close to E2 solubility limit (3000 μg/L) using different water matrices (phosphate buffer and synthetic carbonate buffer). The Michaelis-Menten equation was applied to calculate the three kinetic parameters using Eq. (3) and Eq. (4). The batch degradation experiments were performed by adding 1 mL of the nanobiocatalyst suspension (20 g/L with an initial activity of 20,800 ± 4900 μMol/min.L) to an E2 solution to have a final volume of 100 mL with an enzymatic activity of 197 ± 38 μMol/min.L. The batch reactor (E2 + nanobiocatalyst) was stirred in an incubator shaker (Innova 43 R, New Brunswick Scientific, USA) for 24 hours at 200 rpm and 22.5 ± 0.5 °C. Various samples of 5 mL were taken at specific times (5, 10, 20, 30, 60, 120, 240, 360 and 1440 min) and centrifuged (Centrifuge Sigma 3–16L model, Germany) at 4200 rpm for 2 min in plastic conical vials to precipitate the nanobiocatalyst. A supernatant volume of 3 mL was used for LSC (1 mL) and UHPLC (2 mL) analysis. The nanobiocatalyst was re-suspended in the remaining supernatant and added back to the reactor flask.

2.10. Steroid hormone degradation in filtration experiments

The micro-CF system in flow-through mode was used to evaluate E2 removal by the biocatalytic membranes at environmentally relevant concentrations and different water matrices, as well as the removal of E1, P and T. The filtration was performed with a biocatalytic membrane area of 2 cm^2 and a fixed flow rate of 0.2 mL/min, corresponding to a water flux of 60 L/m^2h and HRT of 4.5 s in the UF-SNPs membrane and 0.6 s in the nanofiber matrix of the nano-MF membrane. HRT was calculated using Eq. (S2). The filtration protocol is described in Table S8. A feed volume of 150 mL containing E2 concentrations of 0.1 μg/L and 3000 μg/L in different water matrices (synthetic carbonate buffer of 10 mM NaCl and 1 mM $NaHCO_3$, a phosphate buffer 0.1 M) was filtered and 100 mL of permeate volume was collected. The filtration was performed at a temperature of 23.2 ± 0.5 °C and an applied feed pressure of 1.1 ± 0.2 bar

3. Results & discussion

Initially, the enzymatic kinetics was evaluated in batch to determine whether the 'speed' of E2 degradation was compatible with the range of HRT and solute flux in a biocatalytic membrane. Subsequently, the enzymatic activity was investigated at different water matrix compositions to determine the inhibition mechanisms of chloride ions, which are usually contained in natural waters.

3.1. Estradiol removal by the nanobiocatalyst in batch and kinetics

E2 removal and kinetics were evaluated in batch to determine the extent of the reaction rate by the nanobiocatalyst, when E2 concentration was increased from a representative environmental concentration of 0.1 μg/L up to a concentration close to the solubility limit (3900 μg/L) (Shareef et al. 2006), in different water matrices. E2 removal as a function of concentration in phosphate buffer and synthetic carbonate buffer (representative of natural water background) is shown in Fig. 3.

The results revealed that E2 removal increased with concentration and the removal was higher in phosphate buffer compared to synthetic carbonate buffer. Indeed, a full removal of 99 % was obtained at concentrations above 100 μg/L in phosphate buffer, while a similar removal was achieved in synthetic carbonate buffer only at higher concentrations of 3000 μg/L, which is close to E2 water solubility limit (3900 μg/L) (Shareef et al. 2006). E2 removal in phosphate buffer is consistent with a

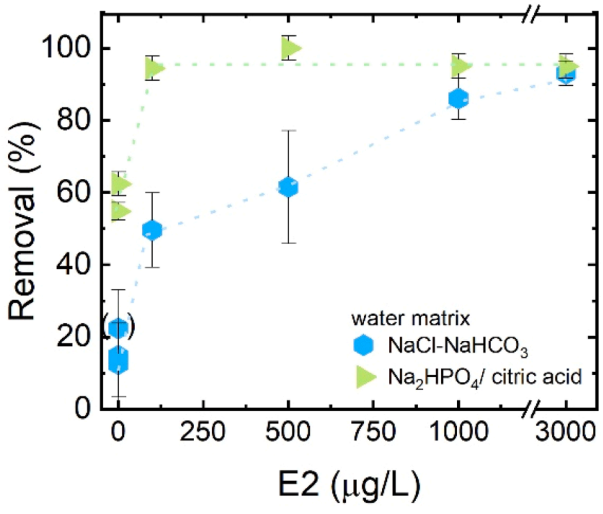

Fig. 3. E2 removal at different E2 concentration in batches (disodium phosphate/citric acid 0.1 M, 10 mM NaCl, 1 mM $NaHCO_3$, pH 5.0 ± 0.1, 22.5 °C, 200 rpm, 24 hours, lac activity 197 ± 38 μMol/min.L, stock SNPs 10 g/L, SNPs mass 10 mg).

previous study (Gamallo et al. 2018), who reported 90 % removal in batch with similar water matrix composition (phosphate buffer and E2 concentration of 3000 μg/L) and nanobiocatalyst (Laccase immobilised on fumed silica nanoparticles). A similar removal of 92 % was reported when Lac Trv was immobilised in a nanofiber matrix and the degradation was performed in batches in phosphate buffer (Zdarta et al. 2022a).

When E2 concentration was decreased to 0.1 μg/L, the removal dropped to 17 ± 7 % and 55 % in synthetic carbonate and phosphate buffer, respectively. The overall trend of E2 removal in batch revealed that E2 degradation by the nanobiocatalyst was influenced by E2 concentration and the water matrix composition. Two hypothesis can be drawn to explain the different removal in phosphate and synthetic carbonate buffer with varying E2 concentration. The first hypothesis is the inhibition of laccase by chloride ions, which can explain the lower removal in the synthetic carbonate buffer. This is supported by previous studies performed with real wastewaters, where a decrease in estrogens removal ranging from 35 to 40 % was reported due to the presence of enzyme inhibitors (e.g. salts, metals, solvents) that can interfere with enzymatic kinetics (Rybarczyk et al. 2023, Zdarta et al. 2022b). The second hypothesis is the slowdown of the reaction kinetics with the decrease in E2 concentration, resulting in lower removal when E2 degradation was performed at realistic environmental concentration. Indeed, previous kinetic studies in batch reactors (Rangelov and Nicell 2015, 2018) reported a lower E2 degradation, when the concentration was decreased by one order of magnitude, which was attributed to slower reaction kinetics.

To elucidate the contribution of E2 concentration and water matrix on the reaction rate by the nanobiocatalyst, kinetic parameters such as the Michaelis-Menten constant (K_M), the maximum apparent rate of disappearance (r'_{max}) and the reaction rate constant (K_r) were calculated. The apparent rate of disappearance as a function of E2 concentration and the kinetic parameters for different water matrix are shown in Fig. 4.

The apparent rate of disappearance increased by four orders of magnitude (from $6{\cdot}10^{-13}$ mol/s.L to $5{\cdot}10^{-9}$ mol/s.L) with the increase of E2 concentration from 0.1 μg/L to 500 μg/L and remained almost constant at $7{\cdot}10^{-9}$ mol/s.L when E2 concentration was further increased to 3000 μg/L in phosphate buffer. A similar trend with a lower rate of disappearance was observed in the synthetic carbonate buffer. The lower rate of disappearance at lower E2 concentration confirms previous reports, where a slowdown of the reaction kinetics for E2 degradation by laccase was observed when the concentration was reduced from 50 to 0.5 μM (Rangelov and Nicell 2015, 2018). It was reported that at very low substrate concentration, laccase can stay in an intermediate resistant oxidized state, which limits the catalytic cycle.

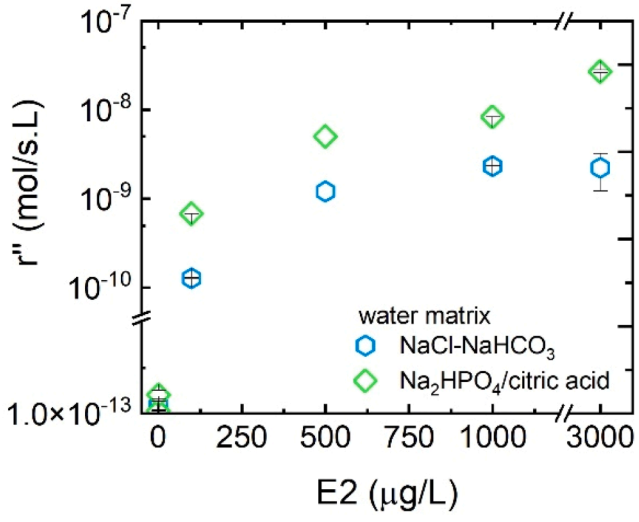

Fig. 4. E2 apparent rate of disappearance in batch at different E2 concentrations (disodium phosphate /citric acid 0.1 M, 10 mM NaCl, 1 mM $NaHCO_3$, pH 5.0 ± 0.1, 22.5 °C, 200 rpm, 24 hours, lac activity 197 ± 38 μMol/min.L, stock SNPs 10 g/L, SNPs mass 10 mg).

The trend shown in Fig. 4 confirms that saturation of the nanobiocatalyst was reached at E2 concentration of 500 μg/L, which is two orders of magnitude higher than the concentration of 0.1 μg/L. According to Michaelis-Menten kinetics, under saturating conditions, the majority of enzyme molecules are complexed with E2 molecules available in solution, and the rate of disappearance becomes independent of E2 concentration (Punekar 2018). This suggests that at environmental concentration of 0.1 μg/L, the nanobiocatalyst is not in the optimal substrate concentration condition to have most laccase molecules complexed with E2, which explains the significant decrease in the apparent rate of disappearance and consequently the lower removal.

To confirm that the lower removal was caused by a reduced rate of disappearance, the reaction rate was compared with the diffusion rate, which was calculated considering the diffusion time, the diffusion surface area in the flask and E2 diffusion coefficient in water (see Eq. S3). A diffusion rate of $1.4{\bullet}10^{-11}$ mol/s.L was obtained, which is about 2 orders of magnitude higher than the reaction rate (or rate of disappearance) calculated at 0.1 μg/L ($6{\bullet}10^{-13}$ mol/s.L). The higher diffusion rate confirms that the biocatalytic oxidation was not limited by diffusion mass transfer at low E2 concentration and the lower removal was caused by the lower rate of disappearance.

To evaluate how the water matrix composition affected the enzymatic kinetics, the kinetic parameters K_M, r'_{max} and the rate constant K_r were determined from the linearised plot of the apparent rate of disappearance as a function of E2 concentration (see Figure S8). The kinetic parameters are listed in Table 2.

Results revealed that r'_{max} at enzymatic saturating conditions decreased by one order of magnitude when the reaction was performed in a synthetic carbonate buffer. This means that the lower E2 removal in the synthetic carbonate buffer was caused by the inhibition of chloride ions, which reduced the apparent rate of disappearance. In contrast, the variation of K_M was within the calculated error for phosphate buffer (0.012 mM corresponding to 3300 μg/L) compared to synthetic carbonate buffer (0.010 mM corresponding to 2730 μg/L), which means that the binding of the laccase catalytic site with E2 was not affected by the water matrix. According to previous studies (Enaud et al. 2011, Raseda et al. 2014), the inhibition of laccase by chloride ions can occur by hindering the electron transfer from the copper T1-Cu to the cluster T2 and T3-Cu, which can limit the accessibility of E2 molecules to the catalytic site (competitive inhibition) or slow down the oxidation reaction by the E2-laccase complex (uncompetitive inhibition). The insignificant variation of K_M suggests that the inhibition was not competitive for the binding to the catalytic site and that chloride ions reduced the reaction rate by binding the complex Lac-E2.

Consistent with the decrease in the apparent rate of disappearance, a reduction in the rate constant (k_r) from $1.8{\cdot}10^{-3}$ 1/s in phosphate buffer to $3.4{\cdot}10^{-4}$ 1/s in a synthetic carbonate buffer indicates that E2 oxidation by the nanobiocatalyst was faster in phosphate than synthetic carbonate buffer (hence the presence of chloride inhibition). A similar result is reported in previous studies where a decrease in the rate constant for E2 oxidation by laccase (range 6.5 to $7.5{\cdot}10^{-4}$ 1/s) was observed in the presence of inhibitors, such as phenolic and humic acid (Liu et al. 2021, Sun et al. 2021). To further confirm that the lower E2

Table 2
Michaelis-Menten parameters for E2 oxidation determined in presence of phosphate and NaCl-$NaHCO_3$ water matrices.

Kinetic parameters	Phosphate buffer	Synthetic carbonate buffer
K_M (mM)	0.012 ± 0.003 (3300 μg/L)	0.010 (2730 μg/L)
r''_{max} (· 10^{-8} mol/s.L)	2.2 ± 0.6	0.3 ± 0.1
K_r (· 10^{-3} 1/s)	1.8	0.3

removal and slower kinetics in synthetic carbonate buffer was caused by the inhibition of chloride ions, the laccase activity was investigated in carbonate and phosphate buffer (Fig. 7) and under different NaCl concentrations (Figure S10). The lower activity in synthetic carbonate buffer and the decreased activity with increasing NaCl concentration demonstrate the dominant inhibition of laccase by chloride ions in synthetic carbonate buffer.

3.2. Estradiol removal by the biocatalytic membrane in filtration

In the second step, E2 removal was investigated using the biocatalytic membrane reactors to evaluate whether the reaction kinetics are compatible with the HRT and solute flux during filtration. E2 breakthrough at different E2 concentrations and water matrices is shown in Fig. 5A and B.

When E2 filtration was performed at concentration of 0.1 μg/L, E2 degradation did not occur as the ratio c_p/c_f remained mostly close to one, indicating no E2 degradation by the biocatalytic membranes irrespective of the water matrices. To explain this result, E2 solute flux and the apparent rate of disappearance for E2 degradation at 0.1 μg/L were compared. Under this concentration, a solute flux in the range of 1.2 mol/s to $1.4{\cdot}10^{-15}$ mol/s for UF-SNPs and nano-MF was obtained, which is about one order of magnitude lower compared to the rate of disappearance determined in batch (range 1.7 mol/s to $6.2{\cdot}10^{-14}$ mol/s). This indicates that the solute flux through the membrane was slower than the reaction rate, hence E2 degradation was limited by solute mass transfer through the membrane.

When the filtration was performed with an increased E2 concentration of about three orders of magnitude (3000 μg/L), a decrease of the c_p/c_f ratio to 0.74 ± 0.08 was observed in both water matrices and for the UF-SNPs membrane, removing 31 % of E2. Increasing E2 concentration (keeping the same water flux) increased the solute flux by four orders of magnitude ($2.5{\cdot}10^{-11}$ mol/s), which is similar to the apparent rate of disappearance obtained in filtration ($1.1{\cdot}10^{-11}$ mol/s). This suggests that at E2 concentration of 3000 μg/L, the solute mass transfer is no longer a limiting factor and E2 degradation by the biocatalytic membrane occurred. This hypothesis is consistent with other studies performed with either biocatalytic membrane reactors or catalytic membranes, where an increase in product formation and rate of disappearance was observed with the increase in solute flux, due to an increase of solute mass transfer, which allowed more substrate molecules to reach the catalytic site (Giorno et al. 2006, Gumí et al. 2008, Lyubimenko et al. 2021).

Surprisingly, when the nano-MF membrane was filtered, a decrease in the c_p/c_f ratio was not observed at the same E2 concentration of 3000 μg/L, although the solute flux ($3.3{\cdot}10^{-11}$ mol/s) was similar to the UF-SNPs membrane. Two main hypotheses were postulated to explain these results: i) different enzyme loading in the membrane porous structure compared to UF-SNPs, ii) different HRT, which is a relevant parameter affecting the performance of a biocatalytic membrane (Ansorge and Staude 1985, Luo et al. 2014). The immobilized mass of enzyme in the UF-SNPs (2 g/m^2) and nano-MF membrane (3 g/m^2) was similar, which is consistent with the similar activity determined with ABTS at the same conditions shown in Fig. 7. The similar enzyme loading could be plausible considering that the non-woven porous structure of the UF support (for the UF-SNPs) and the nanofiber matrix (for the nano-MF) show similar porous structure. This suggests that the insignificant biocatalytic E2 degradation was not caused by a lower enzyme loading. To evaluate the second hypothesis, HRT was compared for the two biocatalytic membranes. Considering the UF support thickness of the sandwich configuration, an HRT of 4.5 s was calculated for the UF-SNPs biocatalytic membrane, which is seven times higher than the HRT in the nanofiber matrix thickness of the nano-MF membrane (0.6 s). This means that the contact between E2 molecules and laccase in the nano-MF membrane was too short for the oxidation . These results suggest that solute mass transfer and HRT were the two main limiting parameters to achieve E2 degradation in the biocatalytic membrane reactors at environmental relevant concentration. While increasing E2 concentration close to the water solubility limit enhanced the solute flux (hence the solute mass transfer) through the membrane, the degradation was not effective in achieving high E2 removal during filtration (31 %). In the next step, the contribution of HRT on laccase activity was investigated to determine whether the enzymatic reaction rate is compatible with the HRT range and water flux typically used in UF/MF.

3.3. Contribution of hydraulic residence time and solute flux on laccase activity

Laccase activity was investigated at different water fluxes spanning the range of UF/MF to determine whether the oxidation rate of the biocatalytic membranes is limited by solute mass transfer and the residence time within the membrane. ABTS removal and rate of disappearance as a function of water flux are illustrated in Fig. 6A and B. The variation of the rate of disappearance with HRT and solute flux is reported in Fig. 6C and D.

For the UF-SNPs membrane, ABTS removal was constant at 78 % in

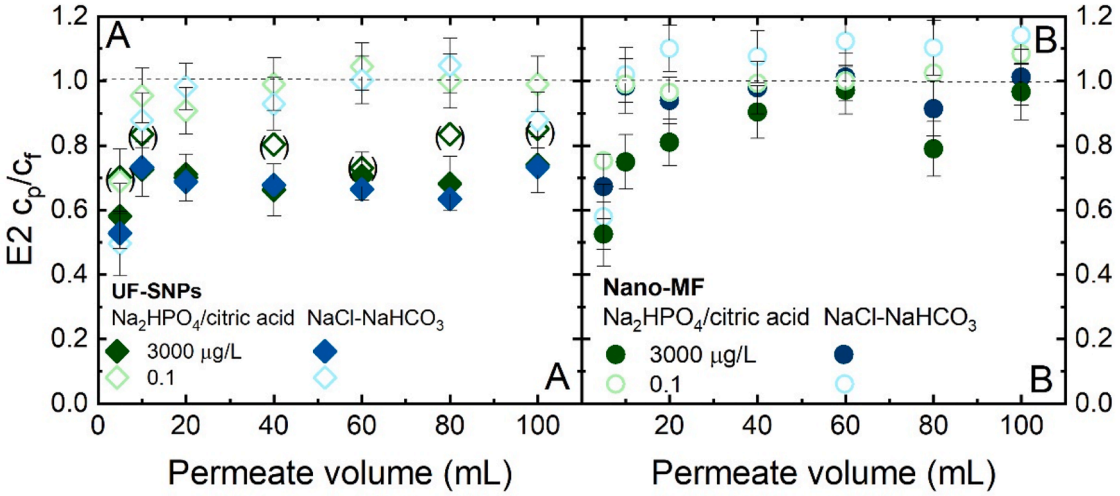

Fig. 5. E2 breakthrough curve as ratio between permeate and feed concentration determined by A) UF-SNPs (SNPs 17 g/m^2 loading), B) nano-MF membranes at different water matrices (10 mM NaCl, 1 mM $NaHCO_3$, disodium phosphate-citric acid 0.1 M, pH 5 ± 0.1) and E2 concentrations (0.1 and 3000 μg/L, 22.7 ± 0.4 °C, 0.2 mL/min, 60 L/m^{2}h, HRT = 4.5 s for UF-SNPs, 0.6 s for nano-MF).

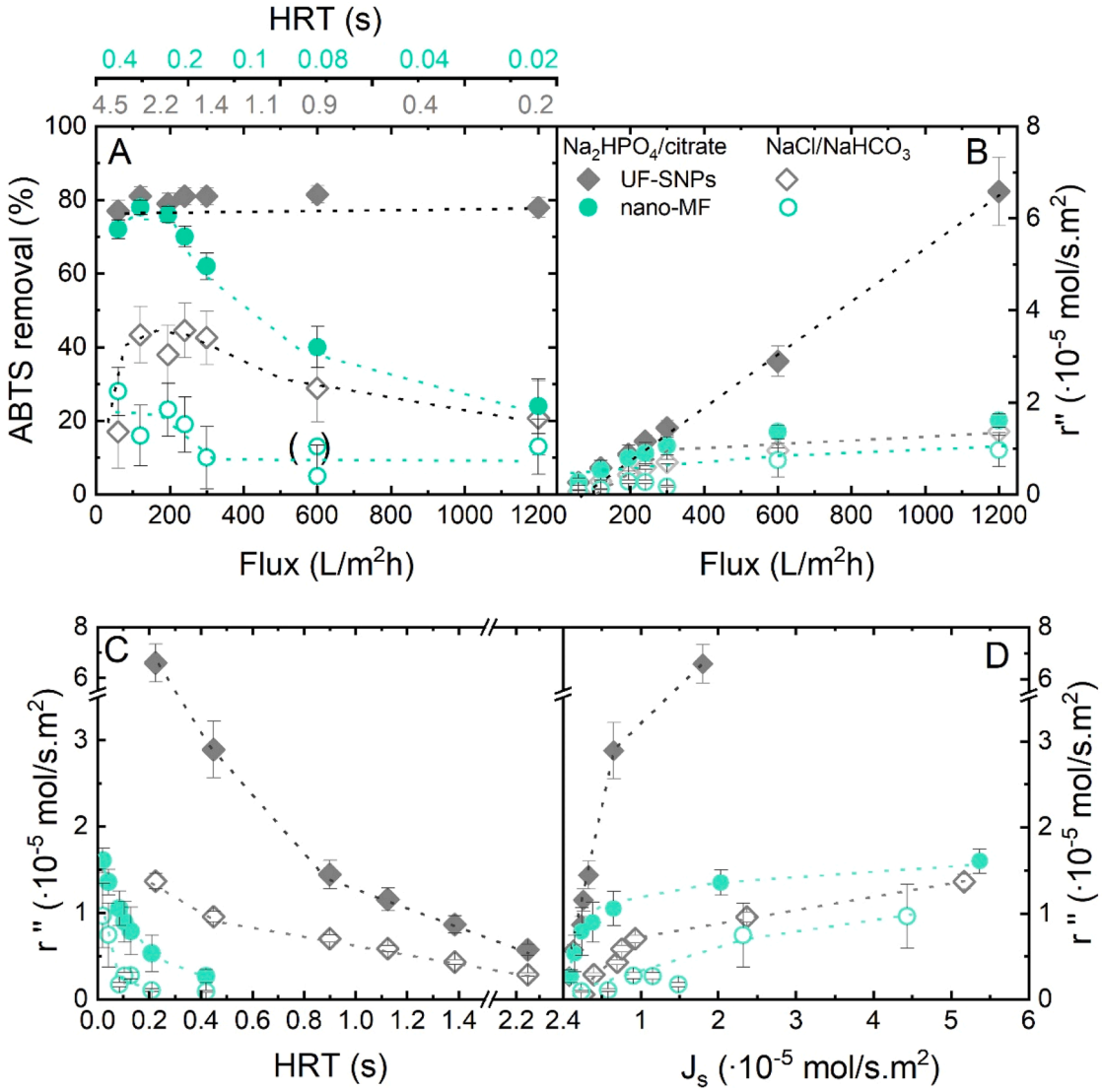

Fig. 6. A) ABTS removal and apparent rate of disappearance as a function of B) water flux, C) hydraulic residence time and D) solute flux by UF-SNPs and nano-MF membranes and different water matrices (10 mM NaCl, 1 mM $NaHCO_3$, disodium phosphate-citric acid 0.1 M, pH 3 ± 0.1, 23.7 ± 0.5 °C, SNPs loading 17 g/m^2, ABTS 0.2 mM).

phosphate buffer, while decreased from 43 % to 21 % with the increase of flux above 300 L/m^2.h and in synthetic carbonate buffer (hence the presence of chlorides) (Fig. 6A). This is consistent with the trend of the rate of disappearance, which increased linearly with water flux in phosphate buffer, while it reached a plateau at flux above 300 L/m^2.h in synthetic carbonate buffer (Fig. 6B). These results indicate that laccase activity was enhanced by the increase of water flux in phosphate buffer, likely due to the increased solute flux, allowing more ABTS molecules to be transported through the UF-SNPs membrane. This hypothesis is confirmed by the trend in Fig. 6D, where the apparent rate of disappearance increased with the solute flux, hence the solute mass transfer. Similar findings are reported in a previous study (Gumí et al. 2008), where it was observed an increase in the butyl laurate permeate flux (the product of the enzyme reaction) with increasing water flux. This was attributed to a higher substrate solute flux, providing more molecules near the enzymatic catalytic site. In another study (Nagy et al. 2015), it was investigated the enzymatic conversion of oleuropein to aglycone in a biocatalytic membrane reactor. It was reported that at shorter residence times and higher water flux, the concentration of oleuropein through the membrane was controlled by the convective flow. Higher conversion to aglycone was observed with longer residence time (> 50 s) and low convective flow (hence water flux).

An opposite trend was observed in synthetic carbonate buffer (Fig. 6B), where the apparent rate of disappearance increased with the solute flux above $1.3 \cdot 10^{-5}$ mol/s.m^2 indicating that at higher flux above 300 L/m^2.h, laccase activity was no longer limited by the solute mass transfer. In this case, the residence time within the membrane became the controlling parameter for the reaction rate as shown in Fig. 6C and D. This is particularly relevant in the presence of inhibitors, such as chloride ions in synthetic carbonate buffer. Indeed, in this case, the ABTS molecules required longer contact time (hence higher HRT and lower flux) to bind the catalytic active site. Previous studies with continuous flow micro-reactors, packed bed reactors and photo and biocatalytic membrane reactors (Cardinal-Watkins and Nicell 2011, Lloret et al. 2013a, Lyubimenko et al. 2021, Vitola et al. 2019) have reported that HRT is a crucial parameter controlling the enzymatic reaction, leading to higher product conversion with longer residence time, which is consistent with the higher rate of disappearance at lower HRT, as depicted in Fig. 6C.

In the case of the nano-MF membrane (Fig. 6A), ABTS removal decreased from 78 % to 24 % and from 23 % to 5 % with the increase of flux above 300 L/m^2.h, in phosphate and synthetic carbonate buffer,

respectively. The apparent rate of disappearance increased to about $1.0{\cdot}10^{-5}$ mol/s.m^2 at higher fluxes without a linear increase as observed for the UF-SNPs membrane. This suggests that in the nano-MF membrane, HRT played a critical part in controlling laccase activity and the reaction rate, independently of the water matrix composition. The apparent rate of disappearance remained almost constant with the increase of solute flux (Fig. 6D), while it increased exponentially by nearly two times when reducing HRT, as shown in Fig. 6C. The results imply that in the presence of inhibitors (e.g. chloride ions in carbonate buffer) and for MF biocatalytic membrane design (i.e. a highly permeable membrane), HRT within the membrane is the dominant parameter controlling laccase activity and consequently the reaction rate. This is especially relevant when the biocatalytic membrane is applied for micropollutant degradation in real natural waters with variable composition, where the presence of inhibitors, such as salts, heavy metals and organic matter (e.g. phenolic and humic acids) can reduce laccase activity or compete with the micropollutant to bind the catalytic site of laccase (Liu et al. 2021, Rybarczyk et al. 2023, Sun et al. 2021).

3.4. Role of water matrix on laccase activity and kinetics

In the next step, laccase activity and kinetic parameters (namely K_M and r'_{max} for ABTS) were determined in phosphate and synthetic carbonate buffer to evaluate how the water matrix affects enzyme affinity (hence the binding of ABTS with the catalytic site) and the reaction rate. ABTS removal and the apparent rate of disappearance at different ABTS concentrations and water matrices are reported in Fig. 7A and B.

For the UF-SNPs membrane, ABTS removal remained unchanged at about 82 % irrespective of ABTS concentration in phosphate buffer, while it decreased from 72 % to negligible removal (<1 %) in synthetic carbonate buffer with decreasing ABTS concentration from 0.5 mM to 0.01 mM (corresponding to 0.02 μg/L) (Fig. 7A). This result specifies that at ABTS concentration close to environmental hormone concentration and in synthetic carbonate buffer, laccase was mostly inactive, and the oxidation rate of ABTS was insignificant. In presence of higher concentration of solvent (e.g. methanol) an insignificant variation of laccase activity was observed in synthetic carbonate buffer (see Figure S11), while decreased significantly by four times at higher NaCl concentration (see Figure S10).

This further confirms the dominant inhibitory effect of chloride ions on laccase in synthetic carbonate buffer and low ABTS concentration. Previous studies investigating the oxidation rate of laccase with ABTS in presence of NaCl reported inhibition of laccase activity by chloride ions, which can bind the catalytic site, hindering substrate reduction, or bind the ABTS-laccase complex, slowing down the enzymatic kinetics (Enaud et al. 2011, Raseda et al. 2014). In synthetic carbonate buffer, NaCl is present at a concentration two orders of magnitude higher (10 mM) than ABTS (0.01 mM), making the dominant inhibition by chloride ions plausible to fully inactivate laccase. By increasing the ABTS concentration by five times (0.05 mM corresponding to 0.1 μg/L), the removal increased to 50 % until it became almost constant at 72 % (close to the removal in phosphate buffer) at ABTS concentrations above 0.4 mM. This trend of ABTS removal suggests that chloride ions might compete with ABTS molecules to bind the catalytic site (competitive inhibition), and the inhibition is mitigated with increasing ABTS concentration.

In case of the nano-MF membrane, ABTS removal was four times lower in synthetic carbonate buffer compared to phosphate buffer, consistent with a lower rate of disappearance, which decreased by three times in synthetic carbonate buffer (Fig. 7B). Interestingly, an opposite trend of ABTS removal was observed with the increase of ABTS concentration in the presence of synthetic carbonate buffer compared to the UF-SNPs membrane. Truly, with the nano-MF membrane, ABTS removal decreased with the increase of ABTS concentration above 0.2 mM from 82 to 54 % and from 27 to 13 % in phosphate and synthetic carbonate buffer, respectively. This trend aligns with the rate of disappearance, which became almost unchanged at ABTS concentrations above 0.2 mM in both water matrices, presenting that laccase saturation was reached at concentrations above 0.2 mM, independently of the water matrix composition. The results shown in Fig. 6C, revealed that in the nano-MF membrane, HRT played a crucial role in controlling the rate of disappearance, hence the time available for ABTS molecules to permeate through the membrane and reach the catalytic site of the enzyme. HRT in the nano-MF was about seven times lower (0.2 s) compared to the UF-SNPs membrane (1.4 s). Hence, the time available for ABTS to overcome the inhibition by chloride ions was insufficient even at higher ABTS concentrations, which can explain the lower removal trend in synthetic carbonate buffer compared to phosphate buffer.

3.5. Inhibition of laccase activity by sodium chloride

To evaluate the inhibition mechanism by chloride ions, the Michaelis-Menten parameters (K_M and r'_{max}) were determined, and the values are reported in Table 3. The linearised plot and inhibition mechanisms are illustrated in Fig. 8.

The variation in kinetic parameters revealed a different inhibition mechanism of chloride ions for UF-SNPs and nano-MF membranes. Indeed, in the case of the UF-SNPs membrane, an increase in K_M of 1.5 times in synthetic carbonate buffer was observed, while the maximum

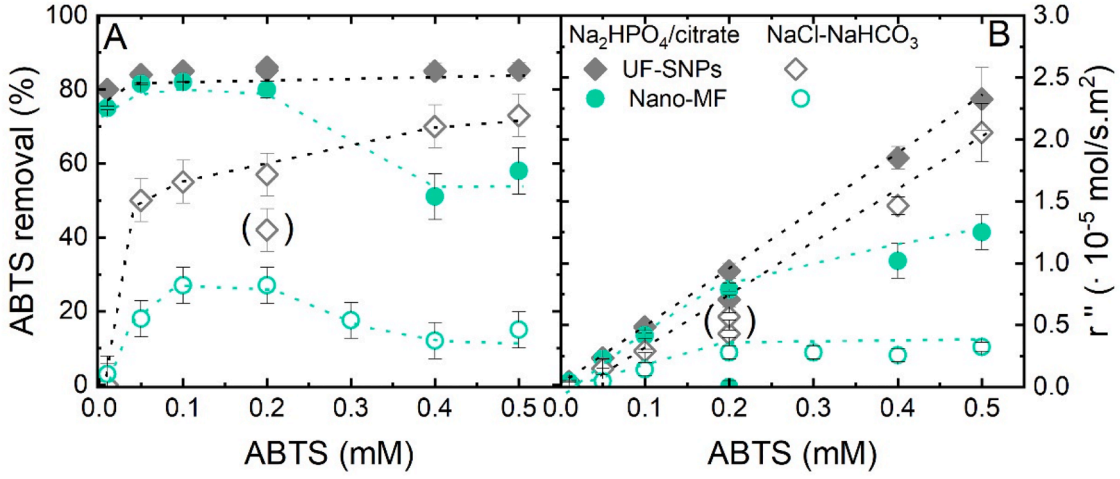

Fig. 7. (A) ABTS removal and (B) apparent rate of disappearance as a function of ABTS concentrations and different water matrices (disodium phosphate/citric acid 0.1 M, 10 mM NaCl, 1mM $NaHCO_3$, pH 3 ± 0.1, 0.65 mL/min, 23.2 ± 0.5 °C, SNPs loading 17 g/m^2) determined with UF-SNPs and Nano-MF membranes.

Table 3
Michaelis-Menten parameters for ABTS oxidation determined in presence of phosphate and synthetic carbonate buffer from the linearized plot in Fig. 8.

Kinetic parameters	UF-SNPs	Nano-MF
$K_{M,\ phosphate}$ (mM)	1.9 ± 0.1	0.5 ± 0.1
$K_{M,NaCl/NaHCO3}$ (mM)	2.8 ± 0.1	0.21 ± 0.03
$r''_{max,\ phosph.}$ ($\cdot 10^{-5}$ mol/s.m^2)	8.3 ± 0.2	2.4 ± 0.3
$r''_{max,NaCl\ NaHCO3}$ ($\cdot 10^{-5}$ mol/s.m^2)	8.3 ± 0.2	0.5 ± 0.1

rate of disappearance remained unchanged. This outcome agrees with the linearised plot in Fig. 8, where the slope of the fit did not change with the water matrix. The increase of K_M indicates that chloride ions reduced the enzyme affinity for ABTS, hence the binding strength with the catalytic active site without interfering with the oxidation rate. This is typical of competitive inhibition, as chloride ions prevent the binding of ABTS to the catalytic site of laccase (Raseda et al. 2014). Indeed, by increasing NaCl concentration ABTS removal and apparent rate of disappearance decreased by four times as shown in Figure S10.

In the case of the nano-MF membrane, a decrease of K_M by 2.5 times and r''_{max} by almost five times was observed. This demonstrates that chloride ions increased the affinity of ABTS molecules for the catalytic site while significantly decreasing the oxidation rate. This trend suggests the dominance of uncompetitive inhibition, where the binding of chloride ions occurs only to the enzyme after the formation of the laccase-ABTS complex, without interfering with the binding to the catalytic site of the free enzyme. When chloride ions bind the ABTS-laccase complex, the enzymatic structure and the catalytic site may be rearranged, which strengthens the binding of ABTS to the catalytic site, resulting in higher affinity (Punekar 2018). The dominance of uncompetitive inhibition is further confirmed by the linearised plot, where the fitting lines for both water matrices are parallel, indicating that both kinetic parameters vary (Punekar 2018).

Previous studies have reported a mixed inhibition mechanism of chloride ions for ABTS oxidation by laccase, encompassing competitive and uncompetitive inhibition. In one study (Raseda et al. 2014), it was observed an increase in K_M with rising NaCl concentration, while the reaction rate decreased fourfold, attributed to dominant competitive inhibition by chlorides directly binding to the active site. This result is consistent with the variation of the kinetic parameters observed for the UF-SNPs membrane. Similar findings are confirmed in another study (Enaud et al. 2011), where the inhibition of laccase by chloride ions occurred through interaction with the copper T1-Cu, preventing the binding of ABTS and subsequent electron transfer to the copper tri-nuclear cluster. This reduces the oxidation rate and enzyme affinity, which aligns with the results of the present study. Uncompetitive inhibition is mentioned as another mechanism of chloride ion, occurring through the binding of chloride to the enzyme complexed with ABTS (Champagne et al. 2013, Enaud et al. 2011, Raseda et al. 2014). In this case, the oxidation rate is predominantly reduced.

4. Conclusions

The intention of this research was to elucidate the limitations of steroid hormone micropollutant degradation by different biocatalytic membranes. The enzymatic reaction was performed during filtration using various water matrix compositions and environmentally relevant concentrations of pollutants in ng/L range.

Batch results revealed that the rate of disappearance decreased significantly by four orders of magnitude when E2 concentration approached 0.1 μg/L, with an insignificant removal of 17 % in synthetic carbonate buffer (containing chloride ions) and 55 % removal in phosphate buffer. This highlighted that the reaction kinetics of estradiol at realistic concentrations were drastically reduced, resulting in an insignificant enzymatic reaction in the biocatalytic membrane. The solute flux at the lowest possible water flux of 60 L/m^2.h (corresponding to HRTs of 4.5 s in the UF-SNPs and 0.6 s in the nano-MF membranes) was still one order of magnitude lower than the apparent rate of disappearance. By increasing E2 concentration to 3000 μg/L, removal of 31 % could be achieved with the UF-SNPs membrane as the solute flux approached a similar order of magnitude to the rate of disappearance; hence, the biocatalytic degradation was no longer limited by the solute mass transfer. In contrary, no removal was observed with the nano-MF membrane due to a sevenfold lower residence time compared to the UF-SNPs membrane, despite a similar solute flux. These results revealed that solute flux (hence the solute mass transfer) and HRT were the two main limiting factors for E2 degradation at environmental concentrations and laccase activity, resulting in ineffective biocatalytic degradation of E2 during filtration to achieve high removal.

The water matrix composition (i.e. phosphate and synthetic carbonate buffer containing NaCl) affected the E2 rate of disappearance and laccase activity, resulting in dominant inactivation of laccase, especially when E2 was at environmental concentration, as NaCl concentration was two orders of magnitude higher in the synthetic carbonate buffer. A mixed inhibition mechanism of chloride ions was observed when laccase activity was tested with ABTS substrate. Indeed, competitive inhibition was dominant in the UF-SNPs membrane, while for nano-MF, the inhibition was mostly uncompetitive, meaning that chloride ions bind to the laccase complexed with ABTS.

The results highlight that E2 oxidation by the tested biocatalytic membrane design is not effective for micropollutant removal at realistic concentrations commonly found in surface water, although a partial

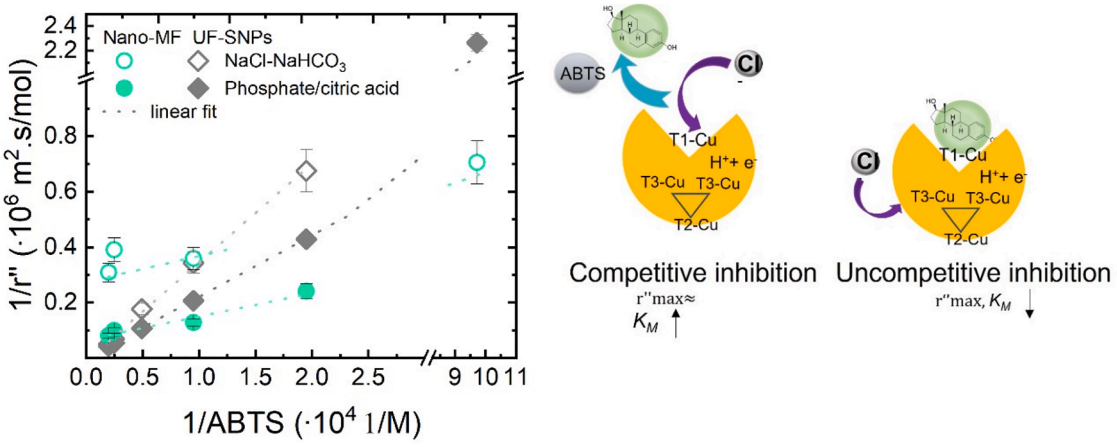

Fig. 8. Lineweaver–Burk plot from linearised Michaelis Menten (disodium phosphate/citric acid 0.1 M, 10 mM NaCl, 1 mM $NaHCO_3$, pH 3 ± 0.1, 0.65 mL/min, 23.2 ± 0.5 °C, SNPs loading 17 g/m^2), schematic of laccase inhibition mechanisms by chloride ions.

degradation could be achieved with the UF-SNPs membrane. This invites further research to enhance the performance of UF-SNPs membrane for the degradation of micropollutants under more realistic natural water compositions. Specifically, future strategies could be directed towards i) accelerating the reaction kinetics at hormone environmental concentrations, for instance, by using enzyme mediators (such as ABTS and 1-hydroxibenzotriazole), which promotes the electron transfer between the oxidized enzyme and E2 molecules, ii) prolonging the residence time within the membrane by loading both UF support of the UF-SNPs membrane, or immobilising the enzyme on an alternative substrate with a high affinity towards the micropollutant.

Supporting information

The supporting information includes a table with an overview of previous studies on the design of biocatalytic membranes for micropollutant degradation with laccase, a section with the description of the nanobiocatalyst preparation, enzyme loading and XPS analysis of the nano-MF membranes and SEM images of the nanofiber matrix cross-section, filtration protocol and a schematic of the filtration system, LSC, UHPLC and UV–vis calibration, ABTS rate of disappearance and removal with different NaCl and methanol concentration, raw data of the filtration and batch reactor experiments, a description of the error analysis.

CRediT authorship contribution statement

Alessandra Imbrogno: Writing – original draft, Visualization, Validation, Project administration, Methodology, Investigation, Funding acquisition, Formal analysis, Data curation, Conceptualization. **Martin Schmidt:** Writing – review & editing, Resources, Methodology. **Agnes Schulze:** Writing – review & editing, Resources, Methodology, Conceptualization. **María Teresa Moreira:** Writing – review & editing, Resources, Methodology. **Andrea I. Schäfer:** Writing – review & editing, Supervision, Resources, Methodology, Funding acquisition.

Declaration of competing interest

The authors declare that they have no known competing financial interests or personal relationships that could have appeared to influence the work reported in this paper.

Acknowledgements

The Helmholtz Association is thanked for the project funding in the form of Recruitment Initiative for IAMT. Millipore (Bedford, USA) provided the UF and MF membranes. The Ministry of Science, Research, and the Arts of Baden-Württemberg is thanked for co-funding of A.I. (Brigitte-Schlieben-Lange-Program). Deutsche Forschungsgemeinschaft (DFG) is thanked for the travel funding in the form of Initiation of International Collaboration (funding number SCHA 1991/6–1 and IM 199/1–1) for the guest visit of Dr. Imbrogno at the University of Santiago De Compostela (USC). The research developed in USC was funded by the project CIES (PID2022-142334OB-I00), granted by the Spanish Ministry of Science and Innovation. Han-ya Lin (IAMT) prepared the electrospun nanofibers of the composite nano-MF membrane and sample preparation for SEM analysis. Sabrina De Boer Rose (University of Santiago de Compostela) engaged in useful discussions on enzymatic kinetics and supported the silica nanobiocatalyst preparation in Spain. Valenzuela Ávila Laura (Department of Chemical Engineering, University of Alcala) and Dr. Jennifer Quirós Jiménez (IAMT) provided SEM images of nano-MF membranes. Prof. Ulbricht and Prof. Giorno contributed inspiring discussions on biocatalytic membrane design and enzyme immobilization.

Supplementary materials

Supplementary material associated with this article can be found, in the online version, at doi:10.1016/j.watres.2024.122902.

Data availability

Data will be made available on request.

References

Adeel, M., Song, X., Wang, Y., Francis, D., Yang, Y., 2017. Environmental impact of estrogens on human, animal and plant life: a critical review. Environ. Int. 99, 107–119.
Ansorge, W., Staude, E., 1985. Kinetic investigations of enzymes covalently bonded to heterogeneous ultrafiltration membranes. J. Membr. Sci. 22 (2-3), 283–295.
Asif, M.B., Hai, F.I., Dhar, B.R., Ngo, H.H., Guo, W., Jegatheesan, V., Price, W.E., Nghiem, L.D., Yamamoto, K., 2018. Impact of simultaneous retention of micropollutants and laccase on micropollutant degradation in enzymatic membrane bioreactor. Biores. Tech. 267, 473–480.
Asif, M.B., Hou, J., Price, W.E., Chen, V., Hai, F.I., 2020. Removal of trace organic contaminants by enzymatic membrane bioreactors: Role of membrane retention and biodegradation. J. Membr. Sci. 611, 118345.
Auriol, M., Filali-Meknassi, Y., Tyagi, R.D., Adams, C.D., 2007. Laccase-catalyzed conversion of natural and synthetic hormones from a municipal wastewater. Water. Res. 41 (15), 3281–3288.
Barbhuiya, N.H., Misra, U., Singh, S.P., 2022. Biocatalytic membranes for combating the challenges of membrane fouling and micropollutants in water purification: A review. Chemosphere 286, 131757.
Beck, S., Berry, E., Duke, S., Milliken, A., Patterson, H., Prewett, D.L., Rae, T.C., Sridhar, V., Wendland, N., Gregory, B.W., 2018. Characterization of Trametes versicolor laccase-catalyzed degradation of estrogenic pollutants: substrate limitation and product identification. Intern. Biodeter. Biodegr. 127, 146–159.
Bilal, M., Barceló, D., Iqbal, H.M., 2021. Occurrence, environmental fate, ecological issues, and redefining of endocrine disruptive estrogens in water resources. Sci. Tot. Env. 800, 149635.
Bilal, M., Iqbal, H.M., 2019. Persistence and impact of steroidal estrogens on the environment and their laccase-assisted removal. Sci. Tot. Env. 690, 447–459.
Bilal, M., Rasheed, T., Zhao, Y., Iqbal, H.M., 2019. Agarose-chitosan hydrogel-immobilized horseradish peroxidase with sustainable bio-catalytic and dye degradation properties. Int. J. Bio. Macromol. 124, 742–749.
Bisswanger, H., 2017. ***Enzyme kinetics: Principles and Methods***. John Wiley & Sons, pp. 55–62.
Bourbonnais, R., Leech, D., Paice, M.G., 1998. Electrochemical analysis of the interactions of laccase mediators with lignin model compounds. Biochim. Biophysica Acta Gen. Subj. 1379 (3), 381–390.
Bridle, H.L., Heringa, M.B., Schäfer, A.I., 2016. Solid-phase microextraction to determine micropollutant-macromolecule partition coefficients. Nat. Protoc. 11 (8), 1328–1344.
Cao, X., Luo, J., Woodley, J.M., Wan, Y., 2016. Bioinspired multifunctional membrane for aquatic micropollutants removal. ACS App. Mat. Interf. 8 (44), 30511–30522.
Cao, X., Luo, J., Woodley, J.M., Wan, Y., 2018. Mussel-inspired co-deposition to enhance bisphenol A removal in a bifacial enzymatic membrane reactor. Chem. Eng. J. 336, 315–324.
Cardinal-Watkins, C., Nicell, J.A., 2011. Enzyme-catalyzed oxidation of 17β-estradiol using immobilized laccase from Trametes versicolor. Enzyme Res. 2011.
Catherine, H., Penninckx, M., Frédéric, D., 2016. Product formation from phenolic compounds removal by laccases: A review. Env Tech. Inn. 5, 250–266.
Champagne, P.-P., Nesheim, M., Ramsay, J., 2013. A mechanism for NaCl inhibition of Reactive Blue 19 decolorization and ABTS oxidation by laccase. App. Microbio. Biotech. 97, 6263–6269.
Chapple, A., Nguyen, L.N., Hai, F.I., Dosseto, A., Rashid, M.H.-O., Oh, S., Price, W.E., Nghiem, L.D., 2019. Impact of inorganic salts on degradation of bisphenol A and diclofenac by crude extracellular enzyme from Pleurotus ostreatus. Biocat. Biotransf. 37 (1), 10–17.
Charni-Natan, M., Aloni-Grinstein, R., Osher, E., Rotter, V., 2019. Liver and steroid hormones—can a touch of p53 make a difference? Front. Endocr. 10, 374.
Dai, Y., Yao, J., Song, Y., Liu, X., Wang, S., Yuan, Y., 2016. Enhanced performance of immobilized laccase in electrospun fibrous membranes by carbon nanotubes modification and its application for bisphenol A removal from water. J. Hazard. Mat. 317, 485–493.
De Cazes, M.d., Belleville, M.-P., Mougel, M., Kellner, H., Sanchez-Marcano, J., 2015. Characterization of laccase-grafted ceramic membranes for pharmaceuticals degradation. J. Membr. Sci. 476, 384–393.
Dong, Z., Tan, J., Pinelo, M., Zhang, H., Wan, Y., Luo, J., 2022. Engineering mussel-inspired coating on membranes for green enzyme immobilization and hyperstable reuse. Ind. Eng. Chem. Res. 61 (15), 5042–5053.
Drioli, E., Giorno, L., 2010. Basic Aspects of Membrane Reactors. Compr. Membr. Sci. Eng. Newnes (ed) 199.
Enaud, E., Trovaslet, M., Naveau, F., Decristoforo, A., Bizet, S., Vanhulle, S., Jolivalt, C., 2011. Laccase chloride inhibition reduction by an anthraquinonic substrate. Enz. Microbial Tech. 49 (6-7), 517–525.

European Parliament Commission implementing decision (EU) 2022/679 of 19 January 2022 establishing a watch list of substances and compounds of concern for water intended for human consumption as provided for in directive (EU) 2020/2184 of the european parliament and of the council (notified under document C(2022) 142).
Gamallo, M., Moldes-Diz, Y., Eibes, G., Feijoo, G., Lema, J., Moreira, M., 2018. Sequential reactors for the removal of endocrine disrupting chemicals by laccase immobilized onto fumed silica microparticles. Biocat. Biotransf. 36 (3), 254–264.
Gebreyohannes, A.Y., Giorno, L., Vankelecom, I.F., Verbiest, T., Aimar, P., 2017. Effect of operational parameters on the performance of a magnetic responsive biocatalytic membrane reactor. Chem. Eng. J. 308, 853–862.
Ghosh, D., Mukherjee, R., 1998. Modeling tyrosinase monooxygenase activity. Spectroscopic and magnetic investigations of products due to reactions between copper (I) complexes of xylyl-based dinucleating ligands and dioxygen: aromatic ring hydroxylation and irreversible oxidation products. Inorg. Chem. 37 (26), 6597–6605.
Giorno, L., Gebreyohannes, A.Y., Drioli, E., Mazzei, R., 2017. Biocatalytic Membranes and Membrane Bioreactors. Compr. Membr. Sci. Eng., Second Edition. Elsevier, Oxford, pp. 55–71.
Giorno, L., Zhang, J., Drioli, E., 2006. Study of mass transfer performance of naproxen acid and ester through a multiphase enzyme-loaded membrane system. J. Membr. Sci. 276 (1-2), 59–67.
Gumí, T., Albacete, J.F.-D., Paolucci-Jeanjean, D., Belleville, M.-P., Rios, G.M., 2008. Study of the influence of the hydrodynamic parameters on the performance of an enzymatic membrane reactor. J. Membr. Sci. 311 (1-2), 147–152.
Hodges, B.C., Cates, E.L., Kim, J.-H., 2018. Challenges and prospects of advanced oxidation water treatment processes using catalytic nanomaterials. Nature Nanotech 13 (8), 642–650.
Imbrogno, A., Schäfer, A.I., 2019. Comparative study of nanofiltration membrane characterization devices of different dimension and configuration (cross flow and dead end). J. Membr. Sci. 585, 67–80.
Jafari, M., Mojtabavi, S., Faramarzi, M.A., Mehrnejad, F., Soleimani, M., Mirjani, R., 2020. Molecular level insight into stability, activity, and structure of Laccase in aqueous ionic liquid and organic solvents: An experimental and computational research. J. Mol. Liquids 317, 113925.
Jahangiri, E., Reichelt, S., Thomas, I., Hausmann, K., Schlosser, D., Schulze, A., 2014. Electron beam-induced immobilization of laccase on porous supports for waste water treatment applications. Molecules. 19 (8), 11860–11882.
Jahangiri, E., Thomas, I., Schulze, A., Seiwert, B., Cabana, H., Schlosser, D., 2018. Characterisation of electron beam irradiation-immobilised laccase for application in wastewater treatment. Sci. Tot. Env. 624, 309–322.
Jankowska, K., Sigurdardóttir, S.B., Zdarta, J., Pinelo, M., 2022a. Co-immobilization and compartmentalization of cholesterol oxidase, glucose oxidase and horseradish peroxidase for improved thermal and H_2O_2 stability. J. Membr. Sci. 662, 121007.
Jankowska, K., Su, Z., Jesionowski, T., Zdarta, J., Pinelo, M., 2023. The impact of electrospinning conditions on the properties of enzymes immobilized on electrospun materials: exploring applications and future perspectives. Env. Tech. Inn., 103408
Jankowska, K., Su, Z., Zdarta, J., Jesionowski, T., Pinelo, M., 2022b. Synergistic action of laccase treatment and membrane filtration during removal of azo dyes in an enzymatic membrane reactor upgraded with electrospun fibers. J. Hazard. Mat. 435, 129071.
Jankowska, K., Su, Z., Zdarta, J., Skiadas, I.V., Woodley, J.M., Pinelo, M., 2024. High performance removal of chlorophenols from an aqueous solution using an enzymatic membrane bioreactor. Env. Poll. 357, 124348.
Khanzada, N.K., Farid, M.U., Kharraz, J.A., Choi, J., Tang, C.Y., Nghiem, L.D., Jang, A., An, A.K., 2020. Removal of organic micropollutants using advanced membrane-based water and wastewater treatment: a review. J. Membr. Sci. 598, 117672.
Kim, Y.-J., Nicell, J.A., 2006. Impact of reaction conditions on the laccase-catalyzed conversion of bisphenol A. Biores. Tech. 97 (12), 1431–1442.
Küchler, A., Yoshimoto, M., Luginbühl, S., Mavelli, F., Walde, P., 2016. Enzymatic reactions in confined environments. Nature Nanotech 11 (5), 409–420.
Kujawska, A., Kiełkowska, U., Atisha, A., Yanful, E., Kujawski, W., 2022. Comparative analysis of separation methods used for the elimination of pharmaceuticals and personal care products (PPCPs) from water–a critical review. Sep. Purif. Tech., 120797
Kumar, A., Sharma, G., Naushad, M., Ala'a, H., Garcia-Penas, A., Mola, G.T., Si, C., Stadler, F.J., 2020. Bio-inspired and biomaterials-based hybrid photocatalysts for environmental detoxification: A review. Chem. Eng. J. 382, 122937.
Levenspiel, O., 1998. Chapter 2. Kinetics of Homogeneous Reactions. ***Chemical Reaction Engineering***, Third Edition. John Wiley & Sons, pp. 13–37.
Li, S., Luo, J., Wan, Y., 2018. Regenerable biocatalytic nanofiltration membrane for aquatic micropollutants removal. J. Membr. Sci. 549, 120–128.
Li, X., Xu, Y., Goh, K., Chong, T.H., Wang, R., 2020. Layer-by-layer assembly based low pressure biocatalytic nanofiltration membranes for micropollutants removal. J. Membr. Sci. 615, 118514.
Lin, Z.-F., Lin, H.-Y., Doong, R.-A., Schäfer, A.I., 2024. Heterostructure g-C_3N_4/Bi_2MoO_6 PVDF nanofiber composite membrane for the photodegradation of steroid hormone micropollutants. J. Hazard. Mat., 134765
Liu, Q., Liu, J., Hong, D., Sun, K., Li, S., Latif, A., Si, X., Si, Y., 2021. Fungal laccase-triggered 17β-estradiol humification kinetics and mechanisms in the presence of humic precursors. J. Hazard. Mat. 412, 125197.
Lloret, L., Eibes, G., Lú-Chau, T., Moreira, M., Feijoo, G., Lema, J., 2010. Laccase-catalyzed degradation of anti-inflammatories and estrogens. Biochem. Eng. J. 51 (3), 124–131.
Lloret, L., Eibes, G., Moreira, M., Feijoo, G., Lema, J., Miyazaki, M., 2013a. Improving the catalytic performance of laccase using a novel continuous-flow microreactor. Chem. Eng. J. 223, 497–506.
Lloret, L., Eibes, G., Moreira, M.T., Feijoo, G., Lema, J.M., 2013b. Removal of estrogenic compounds from filtered secondary wastewater effluent in a continuous enzymatic membrane reactor. Identification of biotransformation products. Env. Sci. Tech. 47 (9), 4536–4543.
Lotfi, S., Fischer, K., Schulze, A., Schäfer, A.I., 2022. Photocatalytic degradation of steroid hormone micropollutants by TiO2-coated polyethersulfone membranes in a continuous flow-through process. Nature Nanotech 17 (4), 417–423.
Luo, J., Meyer, A.S., Jonsson, G., Pinelo, M., 2014. Enzyme immobilization by fouling in ultrafiltration membranes: impact of membrane configuration and type on flux behavior and biocatalytic conversion efficacy. Biochem. Eng. J. 83, 79–89.
Luo, J., Song, S., Zhang, H., Zhang, H., Zhang, J., Wan, Y., 2020. Biocatalytic membrane: Go far beyond enzyme immobilization. Eng. Life Sci. 20 (11), 441–450.
Lyubimenko, R., Busko, D., Richards, B.S., Schäfer, A.I., Turshatov, A., 2019. Efficient photocatalytic removal of methylene blue using a metalloporphyrin-poly (vinylidene fluoride) hybrid membrane in a flow-through reactor. ACS App. Mat. Interf. 11 (35), 31763–31776.
Lyubimenko, R., Cardenas, O.I.G., Turshatov, A., Richards, B.S., Schäfer, A.I., 2021. Photodegradation of steroid-hormone micropollutants in a flow-through membrane reactor coated with Pd (II)-porphyrin. App. Cat. B: Env. 291, 120097.
Lyubimenko, R., Richards, B.S., Turshatov, A., Schäfer, A.I., 2020. Separation and degradation detection of nanogram-per-litre concentrations of radiolabelled steroid hormones using combined liquid chromatography and flow scintillation analysis. Sci. Rep. 10 (1), 1–13.
Margot, J., Bennati-Granier, C., Maillard, J., Blánquez, P., Barry, D.A., Holliger, C., 2013. Bacterial versus fungal laccase: potential for micropollutant degradation. AMB Express. 3, 1–14.
Marpani, F., Luo, J., Mateiu, R.V., Meyer, A.S., Pinelo, M., 2015. In situ formation of a biocatalytic alginate membrane by enhanced concentration polarization. ACS App. Mat. Interf. 7 (32), 17682–17691.
Maryskova, M., Linhartova, L., Novotny, V., Rysova, M., Cajthaml, T., Sevcu, A., 2021. Laccase and horseradish peroxidase for green treatment of phenolic micropollutants in real drinking water and wastewater. Env. Sci. Poll. Res. 28 (24), 31566–31574.
Mazzei, R., Gebreyohannes, A.Y., Poerio, T., Sansone, V., Musteata, V., Upadhyaya, L., Bruno, L., Gorecki, R., Nunes, S.P., Giorno, L., 2024. Dual enzyme compartmentalization in a pH-responsive membrane: a way to tune enzymatic reactions in biocatalytic membranes. J. Membr. Sci. 700, 122708.
Moreira, M.T., Moldes-Diz, Y., Feijoo, S., Eibes, G., Lema, J.M., Feijoo, G., 2017. Formulation of laccase nanobiocatalysts based on ionic and covalent interactions for the enhanced oxidation of phenolic compounds. App. Sciences 7 (8), 851.
Morsi, R., Bilal, M., Iqbal, H.M., Ashraf, S.S., 2020. Laccases and peroxidases: the smart, greener and futuristic biocatalytic tools to mitigate recalcitrant emerging pollutants. Sci. Tot. Env. 714, 136572.
Nagy, E., Dudás, J., Mazzei, R., Drioli, E., Giorno, L., 2015. Description of the diffusive–convective mass transport in a hollow-fiber biphasic biocatalytic membrane reactor. J. Membr. Sci. 482, 144–157.
Nagy, E., Lepossa, A., Prettl, Z., 2012. Mass transfer through a biocatalytic membrane reactor. Ind. Eng. Chem. Res. 51 (4), 1635–1646.
Nguyen, L.N., Hai, F.I., Dosseto, A., Richardson, C., Price, W.E., Nghiem, L.D., 2016. Continuous adsorption and biotransformation of micropollutants by granular activated carbon-bound laccase in a packed-bed enzyme reactor. Biores. Tech. 210, 108–116.
Nguyen, L.N., Hai, F.I., Price, W.E., Kang, J., Leusch, F.D., Roddick, F., van de Merwe, J. P., Magram, S.F., Nghiem, L.D., 2015. Degradation of a broad spectrum of trace organic contaminants by an enzymatic membrane reactor: Complementary role of membrane retention and enzymatic degradation. Intern. Biodeter. Biodegr. 99, 115–122.
Nguyen, M.N., Trinh, P.B., Burkhardt, C.J., Schäfer, A.I., 2021. Incorporation of single-walled carbon nanotubes in ultrafiltration support structure for the removal of steroid hormone micropollutants. Sep. Purif. Technol. 264, 118405.
Nure, J.F., Nkambule, T.T., 2023. The recent advances in adsorption and membrane separation and their hybrid technologies for micropollutants removal from wastewater. J. Ind. Eng. Chem. 126, 92–114.
Omidvar, M., Zdarta, J., Sigurdardóttir, S.B., Pinelo, M., 2021. Mimicking natural strategies to create multi-environment enzymatic reactors: From natural cell compartments to artificial polyelectrolyte reactors. Biotech. Adv., 107798
Popkov, A., Su, Z., Sigurdardóttir, S.B., Luo, J., Malankowska, M., Pinelo, M., 2023. Engineering polyelectrolyte multilayer coatings as a strategy to optimize enzyme immobilization on a membrane support. Biochem. Eng. J., 108838
Punekar, N., 2018. ***Enzymes: catalysis, Kinetics and Mechanism***. Springer, pp. 155–175.
Rangelov, S., Nicell, J.A., 2015. A model of the transient kinetics of laccase-catalyzed oxidation of phenol at micromolar concentrations. Biochem. Eng. J. 99, 1–15.
Rangelov, S., Nicell, J.A., 2018. Modelling the transient kinetics of laccase-catalyzed oxidation of four aqueous phenolic substrates at low concentrations. Biochem. Eng. J. 132, 233–243.
Raseda, N., Hong, S., Kwon, O.Y., Ryu, K., 2014. Kinetic evidence for the interactive inhibition of laccase from Trametes versicolor by pH and chloride. J. Microbio. Biotech. 24 (12), 1673–1678.
Restrepo, M.A., Emonds, S., Zhao, A., Karakas, F., Kamp, J., Roth, H., Wessling, M., 2024. Self-supporting biocatalytic polyelectrolyte complex hollow fiber membranes via salt-dilution induced phase separation. J. Membr. Sci. 689, 122157.
Restrepo, M.A., Kamp, J., Guericke, L., Schnichels, R., Roth, H., Wessling, M., 2023. Single-step polyelectrolyte complex coating on hollow fibers yields nanofiltration or biocatalytic properties. J. Membr. Sci. Lett., 100039
Rybarczyk, A., Smułek, W., Grzywaczyk, A., Kaczorek, E., Jesionowski, T., Nghiem, L.D., Zdarta, J., 2023. 3D printed polylactide scaffolding for laccase immobilization to

improve enzyme stability and estrogen removal from wastewater. Biores. Tech. 381, 129144.
Schmidt, M., Breite, D., Thomas, I., Went, M., Prager, A., Schulze, A., 2018. Polymer membranes for active degradation of complex fouling mixtures. J. Membr. Sci. 563, 481–491.
Schröder, P., Helmreich, B., Škrbić, B., Carballa, M., Papa, M., Pastore, C., Emre, Z., Oehmen, A., Langenhoff, A., Molinos, M., 2016. Status of hormones and painkillers in wastewater effluents across several European states—considerations for the EU watch list concerning estradiols and diclofenac. Environ. Sci. Poll. Res. 23 (13), 12835–12866.
Shakerian, F., Zhao, J., Li, S.-P., 2020. Recent development in the application of immobilized oxidative enzymes for bioremediation of hazardous micropollutants–A review. Chemosphere 239, 124716.
Shareef, A., Angove, M.J., Wells, J.D., Johnson, B.B., 2006. Aqueous solubilities of estrone, 17β-estradiol, 17α-ethynylestradiol, and bisphenol A. J. Chem. Eng. Data 51 (3), 879–881.
Shi, Y., Huang, J., Zeng, G., Cheng, W., Hu, J., 2019. Photocatalytic membrane in water purification: is it stepping closer to be driven by visible light? J. Membr. Sci. 584, 364–392.
Strott, C.A., 2002. Sulfonation and molecular action. Endocr. Reviews 23 (5), 703–732.
Sun, K., Hong, D., Liu, J., Latif, A., Li, S., Chu, G., Qin, W., Si, Y., 2021. Trametes versicolor laccase-assisted oxidative coupling of estrogens: Conversion kinetics, linking mechanisms, and practical applications in water purification. Sci. Tot. Env. 782, 146917.
Vitola, G., Büning, D., Schumacher, J., Mazzei, R., Giorno, L., Ulbricht, M., 2017. Development of a novel immobilization method by using microgels to keep enzyme in hydrated microenvironment in porous hydrophobic membranes. Macromol. Biosci. 17 (5), 1600381.
Vitola, G., Mazzei, R., Poerio, T., Porzio, E., Manco, G., Perrotta, I., Militano, F., Giorno, L., 2019. Biocatalytic membrane reactor development for organophosphates degradation. J. Hazard. Mat. 365, 789–795.
Wang, Y., Chen, Z.-H., 2019. Bioinformatics and enzymatics investigation of Trametes laccase for optical biosensing application. J. Mat. Sci. 54 (6), 4970–4983.
Worch, E., E, 1993. ***Eine Neue Gleichung zur Berechnung von Diffusionskoeffizienten gel&246;ster Stoffe***. VCH, Weinheim.
Wu, C.-C., Shields, J.N., Akemann, C., Meyer, D.N., Connell, M., Baker, B.B., Pitts, D.K., Baker, T.R., 2021. The phenotypic and transcriptomic effects of developmental exposure to nanomolar levels of estrone and bisphenol A in zebrafish. Sci. Tot. Env. 757, 143736.
Xu, F., 1996. Oxidation of phenols, anilines, and benzenethiols by fungal laccases: correlation between activity and redox potentials as well as halide inhibition. Biochemistry 35 (23), 7608–7614.
Zdarta, J., Jankowska, K., Bachosz, K., Degórska, O., Kaźmierczak, K., Nguyen, L.N., Nghiem, L.D., Jesionowski, T., 2021. Enhanced wastewater treatment by immobilized enzymes. Curr. Poll. Reports 7, 167–179.
Zdarta, J., Jankowska, K., Bachosz, K., Kijeńska-Gawrońska, E., Zgoła-Grześkowiak, A., Kaczorek, E., Jesionowski, T., 2020. A promising laccase immobilization using electrospun materials for biocatalytic degradation of tetracycline: effect of process conditions and catalytic pathways. Catal. Today 348, 127–136.
Zdarta, J., Jankowska, K., Strybel, U., Marczak, Ł., Nguyen, L.N., Oleskowicz-Popiel, P., Jesionowski, T., 2022a. Bioremoval of estrogens by laccase immobilized onto polyacrylonitrile/polyethersulfone material: Effect of inhibitors and mediators, process characterization and catalytic pathways determination. J. Hazard. Mat. 432, 128688.
Zdarta, J., Jesionowski, T., Pinelo, M., Meyer, A.S., Iqbal, H.M., Bilal, M., Nguyen, L.N., Nghiem, L.D., 2022b. Free and immobilized biocatalysts for removing micropollutants from water and wastewater: Recent progress and challenges. Biores. Tech. 344, 126201.
Zdarta, J., Sigurdardóttir, S.B., Jankowska, K., Pinelo, M., 2022c. Laccase immobilization in polyelectrolyte multilayer membranes for 17α-ethynylestradiol removal: Biocatalytic approach for pharmaceuticals degradation. Chemosphere 304, 135374.
Zhang, H., Luo, J., Woodley, J.M., Wan, Y., 2021. Confining the motion of enzymes in nanofiltration membrane for efficient and stable removal of micropollutants. Chem. Eng. J. 421, 127870.
Zhao, D., Leth, M.L., Abou Hachem, M., Aziz, I., Jančič, N., Luxbacher, T., Hélix-Nielsen, C., Zhang, W., 2023. Facile fabrication of flexible ceramic nanofibrous membranes for enzyme immobilization and transformation of emerging pollutants. Chem. Eng. J. 451, 138902.
Zimmermann, Y.-S., Shahgaldian, P., Corvini, P.F., Hommes, G., 2011. Sorption-assisted surface conjugation: a way to stabilize laccase enzyme. App. Microbio. Biotech. 92 (1), 169–178.